JOURNAL OF APPLIED POLYMER SCIENCE VOL. 18, PP. 3019–3055 (1974)

Plasticity in Peeling

A. J. DUKE, *Handforth, Cheshire, England*

Synopsis

Contrary to classical theory, a high proportion of bond failures by peeling involve progressive plastic adherend flexural yield. Such yield occurs with adherend thicknesses below a critical value, T_c, which is shown calculable by combining elastic peel mechanics with plastic bending criteria. The geometry of such "peel with yield," and thence the moment-controlled peel forces, can be accounted for only if the adhesive is also recognized as behaving essentially plastically. Subsequent plastic adherend *un*bending is important with highly extensible adhesives. The geometry of "legging" peel in such cases is best described by fully plastic mechanics. These are derived and shown to account for literature data on dependencies of peel force upon peel rate and adhesive thickness. "Stick-slip" peel phenomena are indicated to be controlled by recurring interacting plastic-elastic transitions, in both adhesive and adherend: adhesive strain rate is critical in such phenomena. Four regimes of peel behavior can therefore apply as adherend thickness (T) increases, with peel forces proportional respectively to T^0, $T^{2/3}$, $T^{1/2}$ (above T_c) and finally controlled by moment limitations due to joint configurational constraints ("cleavage").

INTRODUCTION

Theories of peel adhesion (e.g., references 1–4) have generally assumed that the stresses applied to the adherend are less than those which would give rise to inelastic behavior. Because joints are generally weak in peel or cleavage, this is usually true insofar as the tensile force in the peeled adherend is concerned: the adherend tensile yield strength is usually only exceeded during peel at very low angles, when the failure mechanism approximates to that operating during tensile shear joint rupture. However, the peel force exerts a turning moment at the glueline edge, and elastic assumptions also imply that the adherend is so stiff that the maximum values attained by this moment are not such as to cause plastic flexural yield of the adherend, regarded as a cantilever beam. This latter assumption, which has not usually been explicitly stated during the development of peel adhesion theories, but which nevertheless at first sight seems very plausible, proves on examination to be untrue for most practical peel situations.

If the moment at any point along a loaded adherend exceeds the value causing yield in the most highly stressed fibers of the beam, then the localized radius of curvature of the adherend will fall below that as-

Present address: Industrial Chemicals Division, Ciba-Geigy (U.K.) Ltd., Manchester 22, England.

sumed in deriving the elastically based peel mechanics: if the moment attains the fully plastic moment of the beam, M_p, then total collapse occurs with no limitation upon the extent of the irreversible plastic bending of the adherend, unless the moment is reduced by such collapse to a value less than M_p. For idealized adherends of rectangular cross section, having strain-invariant yield stresses for strains beyond yield,[5]

$$M_p = S_y b T^2/4 \tag{1}$$

and the moment at onset of yield is[5]

$$M_y = 2M_p/3. \tag{2}$$

(See Table I for symbols used.)

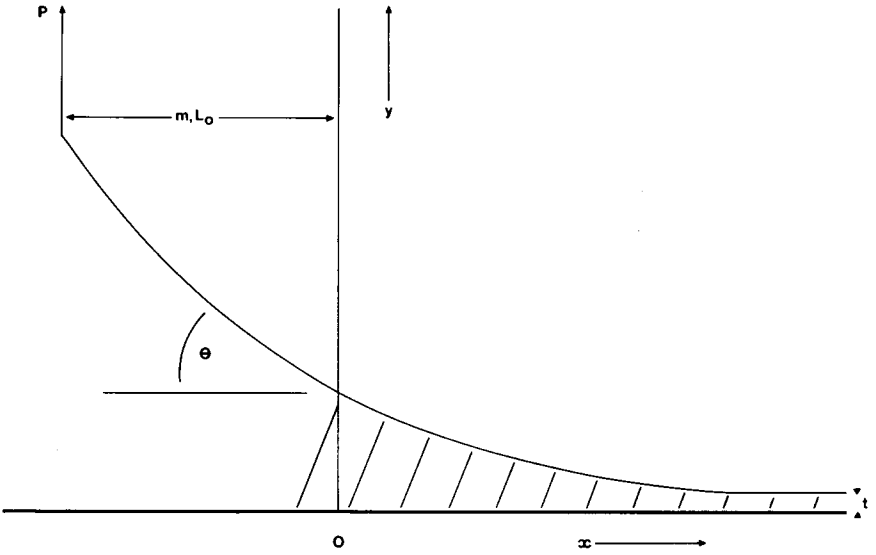

The condition for adherend elastic bending, $M < M_y$ for all points along a loaded adherend, seems to hold only for very stiff adherends or for very weak adhesives. Spies,[1] in his early analysis of peeling, recognized the occurrence of plasticity and tried to allow for it by introduction of an empirically determined "effective" modulus for the adherend. Duke and Stanbridge[6] found that with some structural adhesives, mild steel adherends of thicknesses even up to 3 mm would deform plastically before the joint broke in a cleavage mode: no adhesive in our study was *not* able to cause plastic flexural yield of mild steel around 0.5 mm thick. Mylonas has shown[7] that peel of aluminum foils, as used in conventional peel tests of structural adhesives, proceeds with plastic bending of the peeling adherend, at consequently constant applied moment; and Bickerman[8] has shown that such yield weakens the adjacent glueline edge. The moments at the glueline edge (M_0) implied by the observed peel forces (P) in the studies of Aubrey et al.[9] and of Gent,[10,11] on pressure-sensitive adhesive tapes, are orders of magnitude above M_p if elastic mechanics apply, and in any case imply maximum free moment arms (m) comparable to the adherend thick-

TABLE I
Symbols Used

	Coordinates
x	in bond plane and perpendicular to glueline edge, $x = 0$ at glueline edge on peeling adherend, x positive into unfailed bond
y	perpendicular to bond plane, $y = 0$ at upper boundary of unpeeled adhesive layer
θ	angle of peeling adherend to x axis at $x = 0$
	Dimensions
b	bond width
L	moment arm of P
m	moment arm of peel force
q	length of adhesive zone bearing P
R	radius of adherend curvature
T	adherend thickness
t	adhesive thickness
U	free adherend length
λ	kink wavelength in noisy unwind
	Material Properties
E	adherend Young's modulus
I	adherend moment of inertia, $= b\,T^3/12$
Y	adhesive Young's modulus
β	dimensionless parameter, $= (bY/4EIt)^{1/4}$
	Forces, Stresses, and Strains
F	force exerted in direction of adhesive strain
J	adherend strain
M	moment
P	force applied parallel to y-axis
S	adherend stress
V	normal force applied to an element of adherend
ϵ	adhesive strain
σ	adhesive stress
	Number
f	fractional effective reduced cross section
	Subscripts
C	Wong C region
c	transition from adherend elastic to plastic behavior
E	elastic, or Wong E region
e	effective
f	final
H	around hinge
i	initial
L	due to legs
M_m	for maximum moment
m	maximum
0	around origin (M) or at origin (P)
p	fully plastic
q	around limit of load-bearing zone
u	unloaded (R) or unbending (m)
y	yield
1	lower boundary of plastic unbending zone
2	upper boundary of plastic unbending zone.

TABLE II
Variance Comparisons on Data of Reference 12

		$P \cdot m$	$P \cdot m^2$
11 Results	Means	13.8	20.7
	S.D.	4.1	5.8
	C.V.	30%	28%
9 Results, omitting two most deviant[a]	Means	15.5	20.5
	S.D.	1.7	5.2
	C.V.	11%	25%
	F_8^8	9.4	
	Significance	>99%	
9 Results,[a] normalized to equal means	F_8^8	5.6	
	Significance	~99%	

[a] The two omitted have the two lowest values of $P \cdot m$ and are thus those most likely *not* to have attained a high enough moment to induce plasticity.

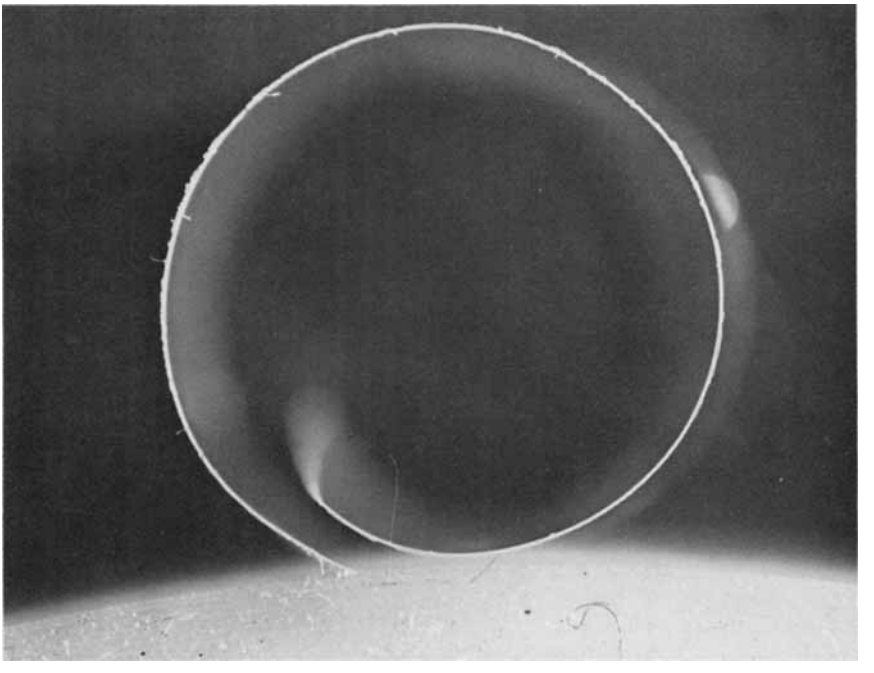

Fig. 1. Photograph of slowly peeled P.S. tape, showing plastic yield.

nesses if M_0 is not to exceed M_p, so that total adherend plastic collapse must apply in peel of such tapes. This has been verified for a cellulosic P.S. tape (Fig. 1), in which the existence of ireversible substrate yield at the glueline edge and along the detached tape is clear after peel over a range of rates. Finally, even the data proffered by Kaelble[12] to support the elastic peel mechanics on analysis (Table II) show much better con-

stancy of $P \cdot m$ than they do of the $P \cdot m^2$ required by the elastic theory, evidently indicating failure at a constant (maximum) moment, limited by the adherend M_p.

Evidently, therefore, elastic peel mechanics can describe only a very limited number of types of peel of practical interest, these being chiefly in the field of cleavage of joints between thick, rigid adherends.

PEEL WITH LIMITED PLASTIC BENDING OF STIFF ADHERENDS

Onset of Plasticity

When a joint peels with plastic flexural collapse of the adherend, such collapse will occur at the (instantaneous) region of highest moment in the loaded adherend. This must lie within the bonded zone, adjacent to that region of adhesive, near the glueline edge, which bears the initial wave of tensile stress.[3] This is because the moment must increase from the point of force application up to the glueline edge, and from some point thereafter (within the bonded zone) must decline to zero, or the whole joint would rotate. From the equilibrium of elements of the bonded adherend in this region, (ref. 4, eq. 6b),

$$dM/dx = V \tag{3}$$

so M_{max} occurs where $V = 0$, and the adherend is transmitting no perpendicular load. (N.B.: This is not the same as the point of no vertical displacement of the adherend, due to the existence of perpendicular forces associated with the restoring moment, within the glueline.)

The equations of the elastic peel mechanics, when used herein, are derived from references 1, 3, 4, and 13. When allowances are made for differences of sign conventions, notation, and definition of dimensionless parameters, the analyses of these four sources appear to be mutally consistent. The sign convention used herein is that adopted by Yurenka,[13] because of the major use which is made of his form of the equations for $(M_0)_m$ (his M_0) and P: only Kaelble use the opposite convention. The notation used herein is defined in Table I; β herein is identical with Kaelble's[3] β and is the reciprocal of Gardon's[4] c (noting that his t_a is twice the t used herein) and of Spies'[1] *second c:* note that Spies redefines c halfway through his analysis, after his eq. (7). Yurenka's[13] equivalent parameter (his β) is not identical with ours, since he works in forces per unit width (his P and I). This usage has not been adopted herein; where applicable, his equations have been rederived by an exactly equivalent analysis to include the bond width b explicitly, and these forms are used for his equations in this analysis.

There are certain critical printing errors in some of the equations of relevance to this analysis. In particular, in Kaelble's[3] eq. (12) in his Appendix I, the second term in the bracket should be $B \sin \beta x$, not $B \cos \beta x$. Yurenka's[13] eqs. (4) and (8) lack β before M, and his eq. (23) lacks

b inside the square root, in each case possibly due to the different method of working mentioned above.

On elastic theory, by combining Kaelble's[3] eqs. (3) and (12) (both from his Appendix I) with $\omega = \pi/2$, adjusting to our sign convention, differentiating, and setting the resulting

$$dM/dx = EI(d^3y/dx^3)$$
$$= e^{-\beta x}(P \cos \beta x - (P + 2\beta M_0) \sin \beta x) \quad (4)$$

to be equal to zero, moment maximum occurs at

$$x_{M_m} = \frac{1}{\beta} \cot^{-1}(1 + 2\beta L_0). \quad (5)$$

This lies halfway between the glueline edge ($x = 0$) and the point of no vertical adherend displacement ($x = \pi/2\beta$, ref. 13) if the peel force is applied directly at the glueline edge ($L_0 = 0$), while $x_{M_m} \rightarrow 0$ (i.e., the locus of maximum moment tends asymptotically toward the glueline edge) as L_0 increases. It is at this point that the adherend develops a "plastic hinge," and as this hinge develops the region of adhesive between it and the glueline edge will be subjected to tensile strains greater than those required of it by elastic theory (and possible also to enhanced shear strains). In consequence, its outer fibers will rupture, the load-bearing capability of the adhesive between the plastic hinge and the glueline edge will decrease, and thus as the free length of adherend rotates about the hinge, reducing m, P is also reduced. The extent of collapse around any one hinge location is thus usually limited, and the hinge shifts progressively along the peeling bond, leaving a permanently bent peeled adherend, of constant radius so long as all other conditions of mode of application of force remain constant (which in practical cases they usually do not).

The full mechanics to describe such "peel with yield" are appallingly complex, even if the adhesive remains elastic, which under the extreme strains imposed by the plastic hinge in the adherend it usually does not. However, a simplification can be applied if L_0 is large enough to allow the approximation that the hinge is at the glueline edge, as applies with the data of reference 6.

From Yurenka's[13] eq. (14),

$$P/P_0 = 1/(1 + \beta L_0) \qquad \text{with } M_0 = PL_0 \quad (6)$$

(deduced on the elastic approximations), the turning moment about the glueline edge (M_0) which can be withstood by a given peeling joint increases monotonically as L_0 increases, P concurrently declining and tending to zero as L_0 tends to infinity. However, his paradoxical limiting case of a joint peeling under a negligible applied force, due to purely moment-controlled adhesive rupture, in practical cases is not attained. This can be due to the (elastic) flexibility of the adherend preventing indefinite increase of the moment arm L_0, and this case is discussed later. However,

even with stiffer adherends another limit prevents the paradox. If $(M_0)_{max}$ exceeds M_p, then either elastic adherend behavior gives way to plastic collapse as L_0 increases for a given joint, or (with lower values of T), adherend plasticity obtains for all L_0, $0 \leqslant L_0 \leqslant M_p/P$. Now, since the elastic mechanics should apply so long as either T is high enough or L_0 low enough, Yurenka's expressions, eq. (6) above, and

$$(M_0)_{max} = P_0/\beta = (EIbt\sigma_m\epsilon_m)^{1/2} \tag{7}$$

permit calculations of adherend thicknesses just allowing plastic adherend collapse and of their dependence upon the initial value of L_0, $(L_0)_i$. We have previously referred to such values of T as T_c and shall do so herein. Since [13] the maximum moment which can be exerted under the elastic mechanics is given by eq. (7), the maximum possible value of T_c, $(T_c)_m$, which applies for high values of L_0, is defined by equating $(M_0)_m$ in eq. (7) to M_y, eq. (2), whence

$$(T_c)_m = 3Et\sigma_m\epsilon_m/S_y^2. \tag{8}$$

If $M_p < (M_0)_m$, then as L_0 increases during (elastic) peel, plastic adherend collapse develops when L_0 becomes of the order of the final radius (R_f) which is attained by the adherend during subsequent stable peeling with yield. Substitution of the (equivalent) conditions

$$L_0 = R_f \tag{9}$$

and

$$M_p = PR_f \tag{10}$$

into eqs. (6) and (7) gives, at the appropriate limit of $R_f \to \infty$, an alternative derivation of eq. (8).

In order to check the validity of eq. (8), some way was required of approximating the *elastic* adhesive "work to rupture product," $\sigma_m\epsilon_m$, from the data for real (inelastic) adhesives. Two such alternative approximations were applied to the data of Duke and Stanbridge,[6] respectively putting $[\sigma_y\epsilon_y + \sigma_m(\epsilon_m - \epsilon_y)]$, or $[\sigma_y\epsilon_y + \epsilon_m(\sigma_m - \sigma_y)]$, in place of $\sigma_m\epsilon_m$ in eq. (8).

The derived $(T_c)_m$ values are plotted against (reassessed) observed T_c ranges in Figure 2. It is reasonable to expect that the observed T_c will be close to this calculated $(T_c)_{max}$, since L_0 (=25 mm) for all cases plotted give values of $\beta L_0 \gg 1$, which is the condition for $M_0 \to (M_0)_m$. The fit of the experimental data is not too bad, particularly as two of the three adhesives which give significantly too low calculated values of T_c themselves show very pronounced inelastic behavior.

En passant, it can be noted that the *minimum* values of T_c, occurring when $L_0 = 0$ and $M_0 = M_p$, which defines the lower bound of T below which *total* plastic collapse occurs for any value of L_0, arises from

$$(M_0)_i = P_0(x_{M_m})L_0 = 0 \geq M_p. \tag{11}$$

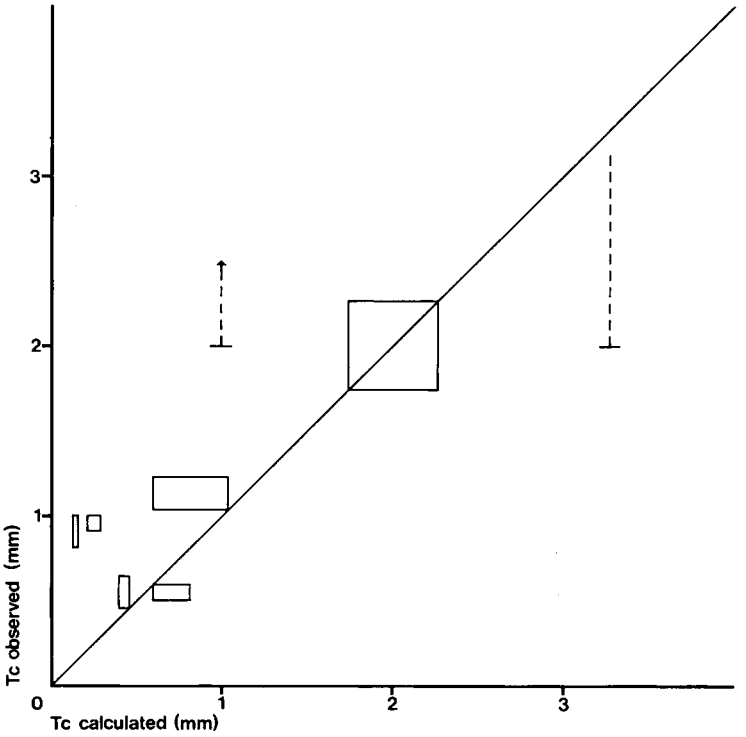

Fig. 2. Plot of observed[6] T_c vs. calculated $(T_c)_{max}$ for eight isotropic adhesives.

Hence, substituting

$$P_0 = b\sigma_m/2\beta \tag{12}$$

from Yurenka's[13] eqs. (11), (17), and (23), and

$$(x_{M_m})_{L_0=0} = \pi/4\beta \tag{13}$$

from eq. (5) herein, then

$$(T_c)_{min} = \pi^2 Et\sigma_m\epsilon_m/12S_y^2 = 0.274(T_c)_{max}. \tag{14}$$

Behavior at this limit was not observed in our previous work,[6] since all adhesives showing high enough $(T_c)_{max}$ values (corresponding to onset of adherend yield with decreasing T) also show high inelastic elongations. With adherends of low T, they therefore exhibit behavior approximating tc legging, vitiating the geometric assumptions underlying Yurenka's theory.[13] T_c for yield initiation, $M_0 = M_y$, should decrease with L_0. When $L_0 = 0$, similarly

$$[(T_c)_{min}]_y = \pi^2(T_c)_{max}/16 = 0.617(T_c)_{max}. \tag{15}$$

However, the decline of T_c from $(T_c)_{max}$ only becomes appreciable at very low values of L_0, in practical cases.

Thus, T_c can be approximately computed from the elastic theory, provided the adhesives are not grossly inelastic.

Peeling Forces in the Plastic Range

When adherend plastic yield occurs, T being $< T_c$, the peeling force is no longer determined primarily by the ability of the adhesive to support tensile loads, but rather by its ability to tolerate the irreversible plastic bending of the adherend in the bonded zone (where $0 \leqslant x \leqslant x_{M_m}$), with consequent reduction in the moment arm m. The uubonded length of adherend then acquires a permanent curvature, radius R_f. During stable "peel with yield," m cannot remain greater than R_f. Thus, since $M_p \geqslant Pm \geqslant M_y$, P has a minimum value, determined by the magnitude of R_f.

Attempts to calculate this second strength-defining parameter from elastic theory are less successful than are calculations of T_c. If, after stable peel with yield has been established, we assume $L_0 \simeq R_f$, eq. (9), then by putting $M_0 = M_y = P R_f$ into eq. (6), and substitting for P_0, eq. (12), and β, we derive

$$\frac{T}{R_f} = \frac{2.28\sigma_m}{S_y}\left(\frac{tE}{TY}\right)^{1/4} - 1.31\left(\frac{TY}{tE}\right)^{1/4}. \tag{16}$$

For the cases where a comparison is possible with our previous data,[6] this relation gives a poor fit to the (empirically near-linear) R_f–T dependence observed (see Fig. 3, lower curves). Equation (16) not only gives generally too low values for R_f, but also predicts a clearly curved R_f–T plot, in

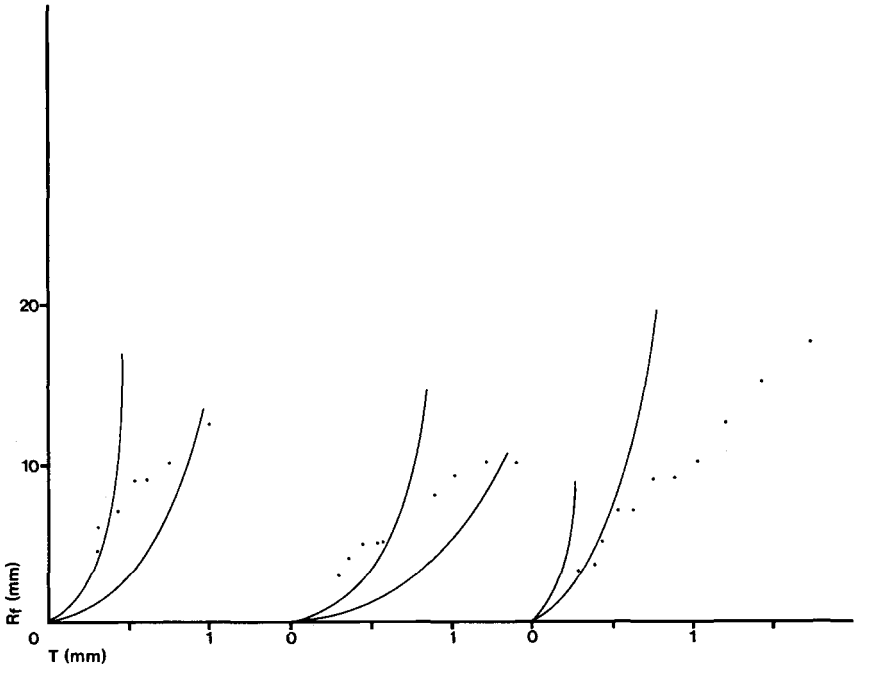

Fig. 3. R_f–T curves calculated for elastic assumptions, for three adhesives of ref. 6, with observed values.

conflict with the facts. The R_f values predicted are higher if M_p is taken in place of M_y in deriving an expression for R_f/T as above, but the predicted curvatures are then even worse (Fig. 3, upper curves).

The three adhesives for which this comparison can be made are all themselves clearly inelastic, and this may have invalidated the above calculation. It may yet apply with any more strictly elastic adhesives which can be found and which give high enough T_c values to permit its verification. However, a simpler approximation gives a much better fit to the observed R_f–T data: we can assume the adhesives also to be fully plastic, at least in the zone $0 \leqslant x \leqslant x_{M_m}$, between glueline edge and plastic hinge, within which the adhesive determines the value of R_f.

As a limit case, we can define "purely plastic" behavior as implying that σ is constant, $= \sigma_y$, for all adhesive elongations > 0. No complete peel mechanics (comparable to the Spies-Jouwersma-Kaelble-Gardon equations) can be derived for such a theoretical adhesive, since integration of the derived beam bending differential equation

$$d^4y/dx^4 = -b\sigma_y/EI \tag{17}$$

in place of the elastic equivalent

$$d^4y/dx^4 = -bYy/EIt \tag{18}$$

(e.g., Kaelble,[3] eq. (8) of his Appendix) must give an undamped quartic, so that the boundary condition of attenuation of strain waves in the adhesive and perpendicular to the adherend, as $x \rightarrow \infty$, cannot be satisfied; furthermore, imaginary compression waves can be predicted from the integration. However, we note that, in elastic mechanics, all of the applied peeling load is balanced by the restoring force in the adhesive between the glue line edge and the point of maximum moment, $0 \leqslant x \leqslant x_{M_m}$. Assume similarly that with a purely plastic adhesive all of the load is borne similarly, by adhesive up to the plastic hinge. Assume further that peel proceeds smoothly and progressively and that the adherend in this zone is cylindrically bent (i.e., that plastic bending proceeds so far at the "hinge" as to give $R_f \ll R_y$).

Then, from the geometry of Figure 4,

$$\epsilon_m t/x_{M_m} = x_{M_m}/2R_f. \tag{19}$$

With the assumed geometry,

$$M_y = Pm = PR_f \tag{20}$$

and with σ_y as defined above,

$$P = b\sigma_y x_{M_m}. \tag{21}$$

Combining eqs. (2), (19), (20), and (21),

$$R_f = (S_y^2/72t\epsilon_m\sigma_y^2)^{1/3}T^{4/3}. \tag{22}$$

Using σ_m for σ_y, this predicts very nearly linear R_f–T plots over the range of T studied and gives excellent fits to our experimental data[6] in four out of the five cases which can be assessed (see Fig. 5). The adhesive in the fifth

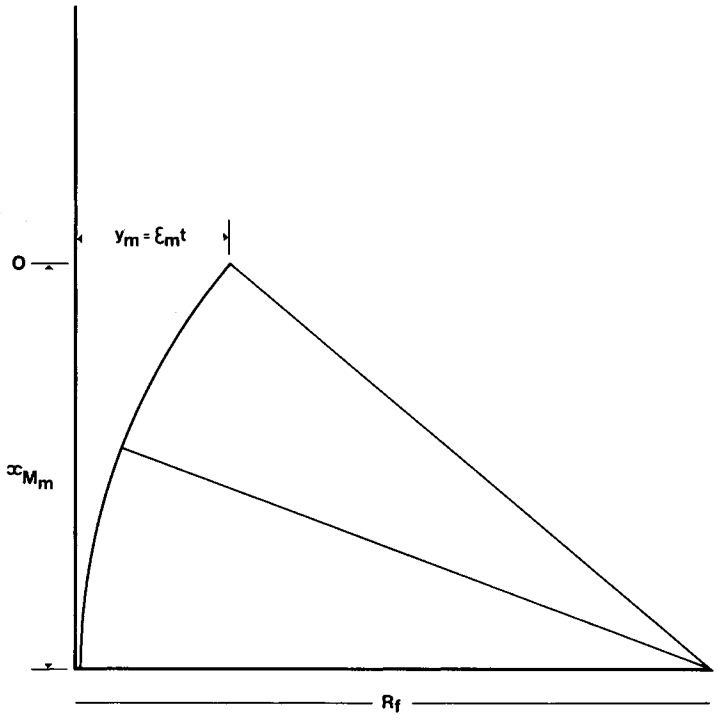

Fig. 4. Geometry of cylindrical adherend bending.

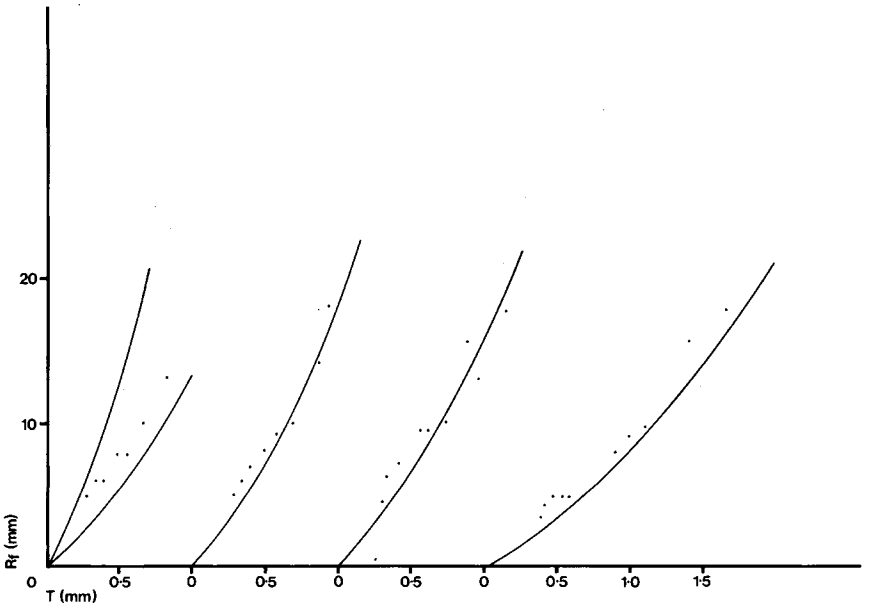

Fig. 5. R_f–T curves for plastic assumptions, with observed data, for four adhesives of ref. 6.

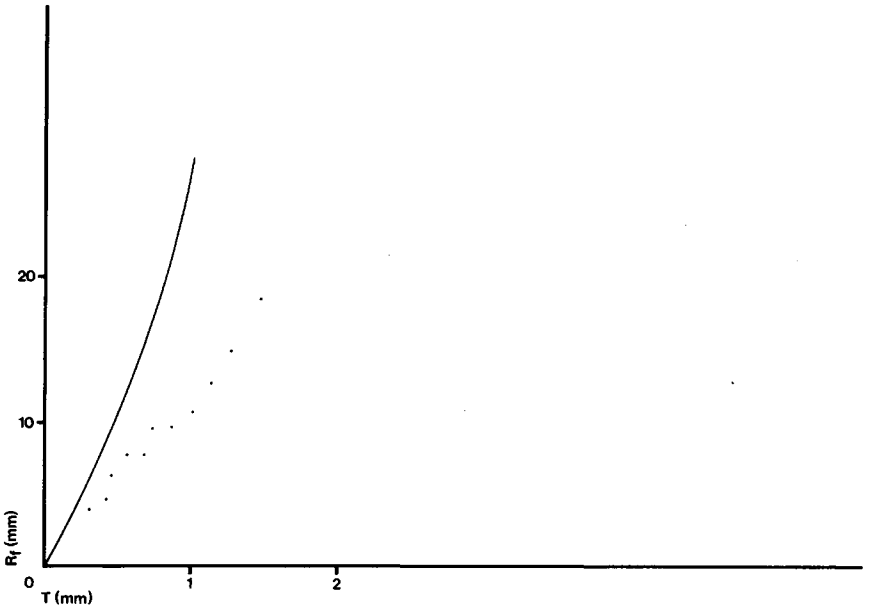

Fig. 6. R_f–T data as in Fig. 5, for a viscoelastic adhesive.

case (Fig. 6) shows viscous rather than plastic behavior, so the appropriate value to use for σ_y in the time scale of the peeling experiments may not have been that determined in our study. For the left-hand plot of Figure 5 (adhesive 9 of ref. 6), our published tensile data conflict with that given (for free adhesive) by the adhesive supplier. In this case, his results may be more reliable than ours. Predicted R_f–T curves for both pairs of ϵ_m and σ_m values are given in Figure 5.

Eliminating R_f between eqs. (20) and (22), we obtain the corresponding equation for the peel force:

$$P = (t\epsilon_m\sigma_y^2 S_y/3)^{1/3} b T^{2/3}. \tag{23}$$

The required dependence of P upon $T^{2/3}$ does seem to be shown for the five adhesives of reference 6 for which several data points are available for the requisite "E type" failures (180° peel-back, so that the required $m \sim R_f$ proportionality holds, $m = 2R_f$). Figure 7 shows that the linear log-log P–T plots for such failures are of mean slope 0.7, as required by eq. (23). This can be contrasted with the dependence of P upon the inverse power of T ($T^{1/2}$) for elastic failures at similarly constant moments, as predicted by Yurenka,[13] eq. (7) herein, and found in reference 6.

The "pure plasticity" assumption for the adhesive thus yields remarkably improved fits to the experimental data over the "elastic adhesive" approximation.

Thus, in cases where peeling with yield occurs smoothly and progressively, without high adhesive ϵ_m permitting legging or otherwise giving high

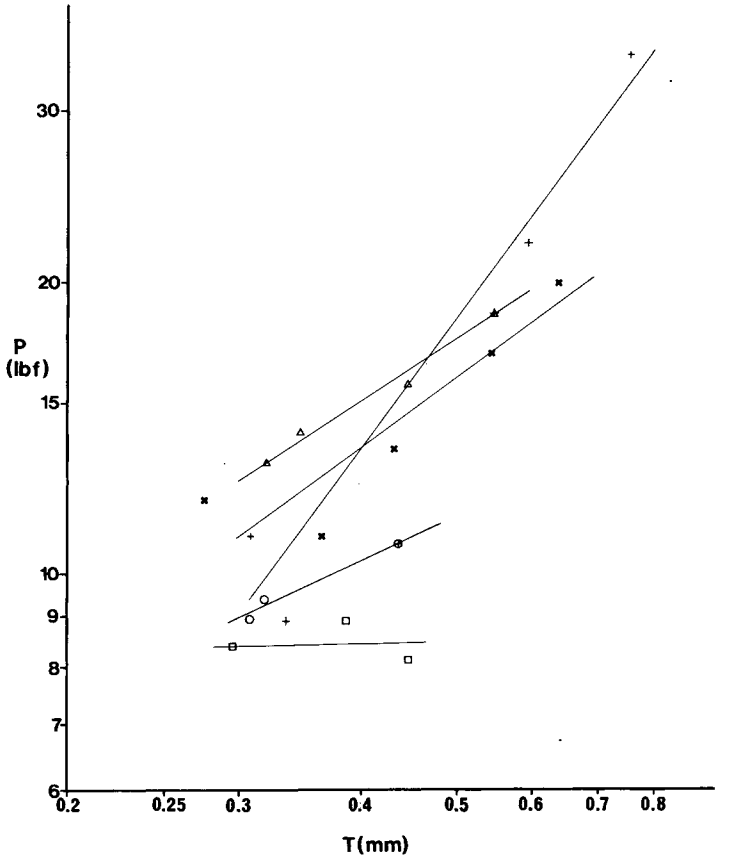

Fig. 7. Log P–log T plots for five adhesives of reference 6, under 180° peel conditions.

angles (θ) between peeling adherend and substrate at $x = 0$, the value of T_c and thus the range of thicknesses for which elastic adherend behavior breaks down, may be determined largely by the elastic characteristics of the adhesive, but thereafter the peeling force (at constant moment, $\approx M_p$) is controlled by more nearly plastic tensile characteristics of the adhesive. Our previous suggestion[6] that adhesive shear strain may control the final bent adherend radius does not give nearly as good a fit to the observed R_f–T data and, in fact, on analysis predicts R_f approximately proportional to T^3 for a plastic adhesive.

The derived type of mechanics can be expected to hold for most adhesive/adherend combinations, provided the adhesive elongations are not too great, say $\epsilon_m < 1$. For more flexible adherends (or long peeling lengths), plastic *un*bending of the free length of the peeled bent adherend may be brought into play as peel proceeds. However, the most usual practical cases in which such unbending is of importance involve adhesives of very high ϵ_m.

PEEL OF HIGHLY FLEXIBLE ADHERENDS BONDED WITH ADHESIVES OF HIGH ELONGATION

Topology

When ϵ_m is significantly larger than 1, many of the assumptions made in deriving the elastic *or* plastic mechanics discussed above (e.g., low θ, adhesive forces parallel to y-axis, no adhesive lateral contractions) break down and a completely different type of mechanics applies. In this, adherends are bent (plastically) back nearly to 90°, and adhesive remains attached to nearly vertical parts of the peeling adherend and thus exerts forces at about 45° to the adherend. As a result, the adhesive can apply enough unbending moment to the adherend in this "legged" region to cause substantial plastic adherend unbending within the bonded zone. In such cases, much of the peeling force is supported by the perpendicular component of the forces applied by adhesive "legs," which are attached to the substrate at points below $x = 0$ and the line of application of force (see Fig. 8). This accounts for the observation, when peeling pressure-sensitive tapes or similar systems, of peel forces much greater than those which could be borne by the available normally stressed adhesive up to the plastic hinge (see Experimental section); the excess force is supported by the legs.

The general form of a peeling joint in such cases is shown in Figure 8. Peeled adherend is still plastically bent to some extent, even after passing through the plastic *un*bending region (y_1 to y_2, Fig. 8), and so each element of the adherend at $y > y_0$ would have a finite "unloaded" radius (R_u) if the applied stresses (and those due to the adhesive) were removed. As a result, whereas the variation of moment with x in classical elastic peel mechanics is independent of the adherend curvature or deflection, in this case the dependence of moment upon y and x is seriously affected by the *un*loaded radii of the various zones of the adherend (which are in turn controlled by the moment distribution). Furthermore, the discontinuities in R which occur for all $M > M_y$, and the absolute limit of $M \not> M_p$, make strict application of continuum mechanics very difficult. The general distribution of R_u is indicated on Figure 8; but, since the locations of points of maximum (positive or negative) moment change with adherend deflection, the exact locations of the zones of plasticity remains to be determined. This is particularly true of the position of the unbending zone relative to the edge of the (legged) bonded zone. Because large components of the forces due to adhesive legs are parallel to the adherend, the displacements along the x-axis which result from even small changes in adherend curvature (particularly for $y > y_1$) can give rise to significant changes in the moments due to the legs. Adherend curvature is influenced both by R_u and by the locally applied moment. The general adherend topology, therefore, has to be assessed before even simplified calculations can be attempted.

Note first that, empirically, the finally detached adherend is not completely straightened by plastic unbending (see, e.g., Fig. 1). That is, $(R_u)_f < \infty$. and therefore $0 < x_f$ (but $< x_{M_m}$: the latter inequality is

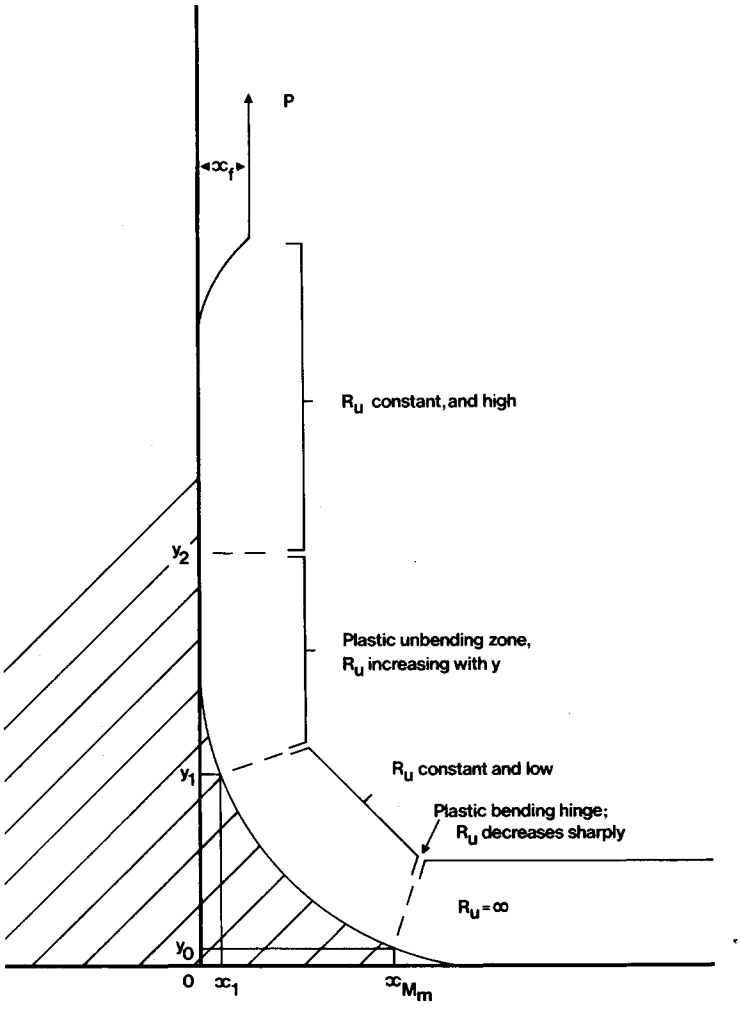

Fig. 8. Form of peel for high ϵ_m.

required for a bending moment at x_{M_m}). The moment due to P reinforces that due to the legs (unbending) so long as $x < x_f$ and opposes it when $x > x_f$. The integrated unbending moment due to all adhesive legs on the high-y side of any point must increase monotonically as y tends to zero from y_m (the value of y at the edge of the legged adhesive zone, whose magnitude relative to y_1 and y_2 is as yet undefined), unless the adherend ever bends so far that its angle to the y-axis exceeds that made by its adjacent legs. This latter seems a most improbable contingency and is certainly not observed experimentally. Furthermore, as the adherend diverges from $x = 0$ toward x_{M_m} with decreasing y, the unbending moment contributed by the horizontal component of the leg's forces is augmented

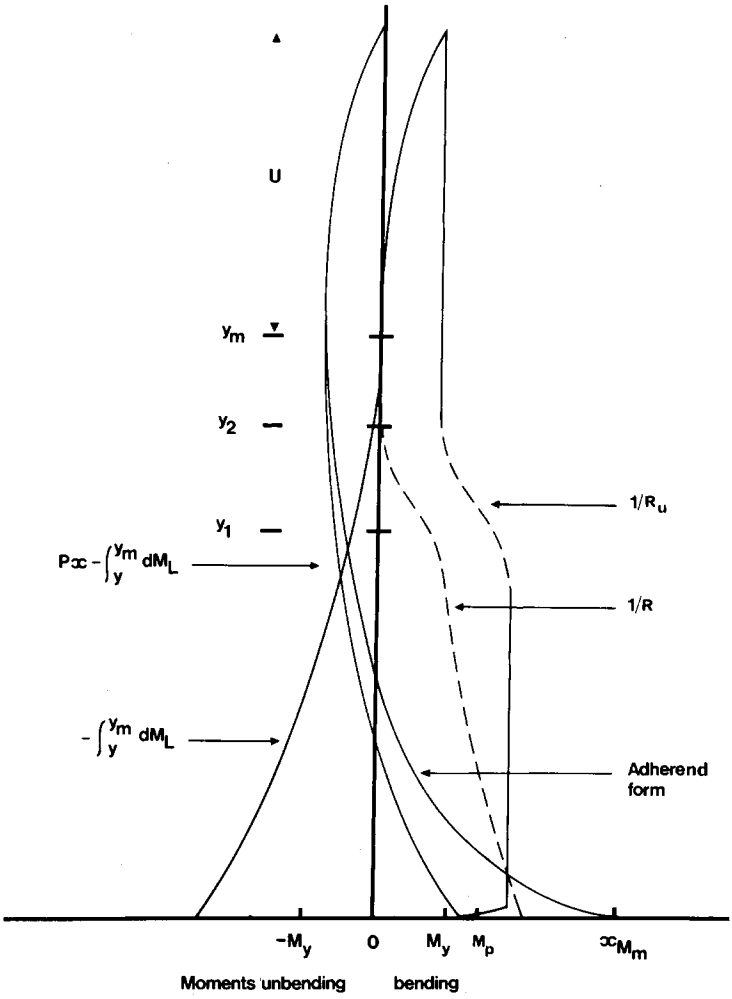

Fig. 9. Schematic variations of adhesive form and curvature and of moment distributions in a joint as in Fig. 8.

increasingly by contributions from the vertical components of the leg forces.

$(R_u)_f$ does not seem empirically to depend on the free adherend length (Fig. 1), which for peeling tapes is usually large relative to y_m. P is also substantially independent of the free length; and thus, since the moment required to (elastically) unbend the curve of radius $(R_u)_f$ along the undefined length of free adherend is a constant, x_f is independent of the free adherend length. R equals $(R_u)_f$ at the point of application of the peeling force, rapidly rises as y decreases therefrom until $R \rightarrow \infty$, and (if the free length is adequate) the adherend remains substantially linear and parallel to the y-axis thereafter up to the region of y_m. Thus, although the peel

force alone provides an unbending moment of up to $P \cdot x_f$, this is smaller than M_y, and no plastic unbending occurs outside the bonded (or legged) zone.

It is not known *ab initio* whether y_m is greater or less than y_2, but we can write the moment applied due to P at y_m as M_0, as in the classical theory (although here M_0 is an unbending, not a bending, moment). The $(dx/dy)_{y_m}$ value, if positive, can be indefinitely small, but it can in principle be negative. If we write the (unbending) moment due to the legs attached to a vertical element of adherend dy as dM_L, then for any y, $y_m > y > 0$, the bending moment is given by

$$M = P(x - x_f) - \int_y^{y_m} dM_L. \tag{24}$$

For this to have a minimum, as y decreases, x must be increasing, and x must increase faster than $\left(\int_y^{y_m} dM_L\right)\Big/P$ on the low-y side of the minimum, but slower on the high-y side.

Unbending may occur over an extended range, so that $y_1 \not\equiv y_2$ in Figure 8. For $y_2 \geqslant y \geqslant y_1$, $M_y \leqslant -M < M_p$, and R_u increases continuously and smoothly with y, but nevertheless not so quickly as to produce a reverse (loaded) curvature at any point, nor thus any consequential increase of (negative) slope dx/dy as y increases. The decrease in R_u at substantially constant moment causes x to increase at an increasing rate as y decreases from y_2 to y_1 (and thereafter), so that M ultimately rises to become algebraically greater than $-M_y$ for $y < y_1$, and finally to $+M_y \leqslant M \leqslant M_p$ at y_0. The interdependent variations of curvatures $(1/R)$, moment and adherend form, as deduced, are given schematically in Figure 9.

Analysis

Since the overall configuration of the adherend is controlled by the relative positions of its plastic zones, location of these is the next requirement of any analysis of such a peeling situation. For a first approximation, assume that, y_m being larger than x_{M_m} and the angle of the adherend to x-axis at x_{M_m} being high, all legs are at 45° to the x- and y-axes. The force (F_L) exerted by the legs attached to an element of adherend, dy $(= dx)$, which legs are of fractional reduced effective cross-sectional area f, is

$$F_L = f\,\sigma_y b\,dx \tag{25}$$

(exerted in the direction of the leg), if the adhesive is "purely plastic" in the sense previously used. Alternatively, if the adhesive is elastic and we also assume that, for the points of attachment of the two ends of the leg, at $(x_L,0)$ and at y_L on the free adherend, $y_L = x_{M_m} - x_L$ (i.e., as above, that the adherend after the plastic hinge immediately becomes effectively vertical, with the legs at 45°), then

$$F_L = \sqrt{2} \cdot fYyb\,dx/t. \tag{26}$$

Obviously, $f < 1$ for any $y > 0$, and two alternative simple and plausible assumptions are a linear decrease of f, from 1 at $y = 0$ to zero at $y = y_m$, i.e.,

$$f = 1 - (y/y_m) \tag{27}$$

or constant adhesive volume with cross-sectional area constant along leg length

$$f = t/[(y + t)\sqrt{2}]. \tag{28}$$

Empirically,[14] F_L is invariant or decreases somewhat as y increases from 0 to y_m, but $F_L \not\to 0$ as $y \to y_m$. Assumption (27) for f is, therefore, inadmissible for either plastic or elastic adhesives: in the former case, (25), it results in F_L tending linearly to zero as $y \to y_m$, and in the latter, (26), in $F_L = 0$ at both $y = 0$ and $y = y_m$, in each case in gross conflict with Kaelble's experimental results.[14] Substitution of the preferred assumption for f, eq. (28), into eq. (25) leads, for a plastic adhesive, to

$$F_L = \sigma_y bt\, dx/(y + t)\sqrt{2}. \tag{29}$$

In eq. (26), for an elastic adhesive, (28) yields

$$F_L = Yyb\, dx/(y + t) \doteq Yb\, dx \tag{30}$$

(since $y \gg t$ for the majority of the legs). The approximation made in the latter case cannot be applied in the former without producing the ludicrous result $F_L = \infty$ at $y = 0$. Even in the latter case, it results in F_L being finite for $y = 0$, but as legs near to $y = 0$ have little effect on moment distributions, the effect of this anomaly is not great, and anyway, Kaelble's results[14] suggest a maximum for F_L near to the point of cavitation to form legs where y starts to increase rapidly (i.e., at the plastic hinge.)

The true form for F_L is probably somewhere between the purely plastic and the elastic approximate forms: Kaelble's F_L traces[14] decline toward the edge of the legs region, but not as rapidly as is implied by the *purely* plastic form for F_L; i.e.,

$$(F_L)_i/(F_L)_f = (y_m/t) + 1. \tag{31}$$

One final minor simplification is made, that $x = 0$ for all $y_m \geqslant y \geqslant y_2$, that is, that the peeled adherend remains straight and vertical once clear of the plastic unbending zone, at least until it is completely unbonded. In fact, it seems likely that unbending occurs very close to the glueline edge, i.e., that $y_2 \doteq y_m$, at least for long free adherend lengths, when $(dx/dy)_{0,y_m} \doteq 0$. This is because the unbending moment contributed by legs between y_2 and y_m must otherwise rapidly give rise to a reversed curvature as y decreases. Such reversed curvature is very infrequently (if ever) observed. Hence, M_0 is not much less than M_y.

When the free length of adherend is long, it follows that R_f is that radius which can just be elastically unbent by M_y. Inserting this in the Bernoulli-Euler equation,[15]

$$M_y = EI/R_f. \tag{32}$$

substituting eq. (2) and for I, gives

$$R_f = ET/2S_y. \tag{33}$$

This equation seems to hold fairly well. For the P.S. tape used in the experimental herein, it indicates that $R_f \doteq 2^1/_2$ mm. The observed value (as in Fig. 1) is circa 4 mm.

Resolving F_L into components parallel to the axes, for the elastic case, from (30) (noting that, since the legs are at 45° to the axes, $dx = dy$),

$$P = \int_0^{y_m} Yb\, dy/\sqrt{2} = Yb\, y_m/\sqrt{2} \tag{34}$$

and the bending moment at x_{M_m} is given by the summation

$$M_p = P\, x_{M_m} - M_0 - \int_0^{y_m} Yby\, dy/\sqrt{2} - \int_{y_2}^{y_m} Yb\, x_{M_m} dy/\sqrt{2} - \int_0^{y_2} Yb\, m_x dy/\sqrt{2} \tag{35}$$

in which m_x is the moment arm about x_{M_m} exerted by the vertical component of F_L for $y < y_1$. Since the angle of the adherend to substrate for $y_2 > y > 0$ is steep, we approximate this length as linear,

$$m_x = x_{M_m} y/y_2. \tag{36}$$

Inserting (36) into (35) and integrating,

$$M_p + M_0 = Yb(x_{M_m} y_2 - y_m^2)/2\sqrt{2}. \tag{37}$$

This must be positive, and thus even if y_2 is as great as y_m, x_{M_m} must be larger than y_m, which does not accord with the geometrical assumptions made, nor with the common observations (e.g., ref. 9) of peeling with legging at near 90° angle, with $x_{M_m} < y_m$.

Calculations for a plastic adhesive, however, yield more plausible results. Proceeding as before, from eq. (29)

$$P = \int_0^{y_m} \sigma_y bt\, dy/2(y + t) = \frac{\sigma_y bt}{2} \ln\left(\frac{y_m}{t} + 1\right) \tag{38}$$

(plus, strictly, a component supported by adhesive from $x = 0$ to x_{M_m}, wherein $y \approx 0$), and the bending moment around $(x_{M_m}, 0)$ is, similarly,

$$M_p = P\, x_{M_m} - M_0 - \int_0^{y_m} \sigma_y bty\, dy/2(y + t) - \int_{y_2}^{y_m} \sigma_y bt\, x_{M_m} dy/2(y + t) - \int_0^{y_2} \sigma_y bt\, m_x\, dy/2(y + t). \tag{39}$$

Substituting for m_x and simplifying the integrations by noting that over most of the range of integration $y \gg t$ so that $(y + t) \to y$,

$$M_p + M_0 = \frac{\sigma_y bt}{2}\left(x_{M_m} \ln\left(\frac{y_m}{t} + 1\right) - y_m - x_{M_m} \ln\left(\frac{y_m + t}{y_2 + t}\right) - x_{M_m}\right). \tag{40}$$

(Since y_2 is $\ll y_m$, the third term can be ignored.) Also, for the unbending moment at y_2, from eq. (29)

$$M_y = M_0 + \int_{y_2}^{y_m} \sigma_y bt(y - y_2)\, dy/2y \tag{41}$$

whence, integrating,

$$M_y - M_0 = \frac{\sigma_y bt}{2} (y_m - y_2 - y_2 \ln (y_m/y_2)). \tag{42}$$

Adding the two moment sum integrals (40) and (42),

$$M_p + M_y = \frac{\sigma_y bt}{2} \left(x_{M_m} \ln \left(\frac{y_m}{t} + 1 \right) - y_2 \ln (y_m/y_2) - x_{M_m} - y_2 \right). \tag{43}$$

This sum must be positive. Since the minimum value for the second term is zero (when $y_2 = y_m$), therefore

$$x_{M_m} \left(\ln \left(\frac{y_2}{t} + 1 \right) - 1 \right) > y_2 \tag{44}$$

and hence also $y_2 > t\,(\mathrm{e} - 1)$, which is in general accord with the proposed geometry. [Relation (44) arises more directly if we assume $y_2 = y_m$ and thus also $M_0 = M_y$ in eq. (40).]

Since, adding eqs. (1) and (2),

$$M_p + M_y = 5S_y bT^2/12 \tag{45}$$

relations (43) and (44) define the dependency of x_{M_m} upon ϵ_m $(= \sqrt{2} \cdot y_m/t)$. Since σ_m is not as readily defined as is P for cases where data are available, we eliminate the former from (43) in terms of the latter. At $y_2 = y_m$, combining eqs (38), (43), and (45),

$$5S_y b\, T^2/12 = P \left\{ x_{M_m} \left[\ln \left(\frac{y_m}{t} + 1 \right) - 1 \right] - y_m \right\} \Big/ \ln \left(\frac{y_m}{t} + 1 \right) \tag{46}$$

or, rearranging,

$$x_{M_m} = \left(5S_y b\, T^2 \left[\ln \left(\frac{y_m}{t} + 1 \right) \right] \Big/ 12P + y_m \right) \Big/ \left(\ln \left(\frac{y_m}{t} + 1 \right) - 1 \right). \tag{47}$$

For the first term in the numerator of this expression to be significant, the adherend has to be fairly stiff. For the data of Aubrey et al.,[9] Gent,[10,11] and of the experimental section herein, this first term can be neglected, and

$$x_{M_m} = y_m \Big/ \left[\ln \left(\frac{y_m}{t} + 1 \right) - 1 \right]. \tag{48}$$

Equation (48) is plotted, in terms of the dimensionless ratios x_{M_m}/t and $y_m/t = \epsilon_m/\sqrt{2}$, in Figure 10, which shows that as the adhesive failure elongation ϵ_m increases from its limit minimum of $\sqrt{2}(\mathrm{e} - 1)$, x_{M_m} passes through a minumum and thereafter increases more slowly than does y_m.

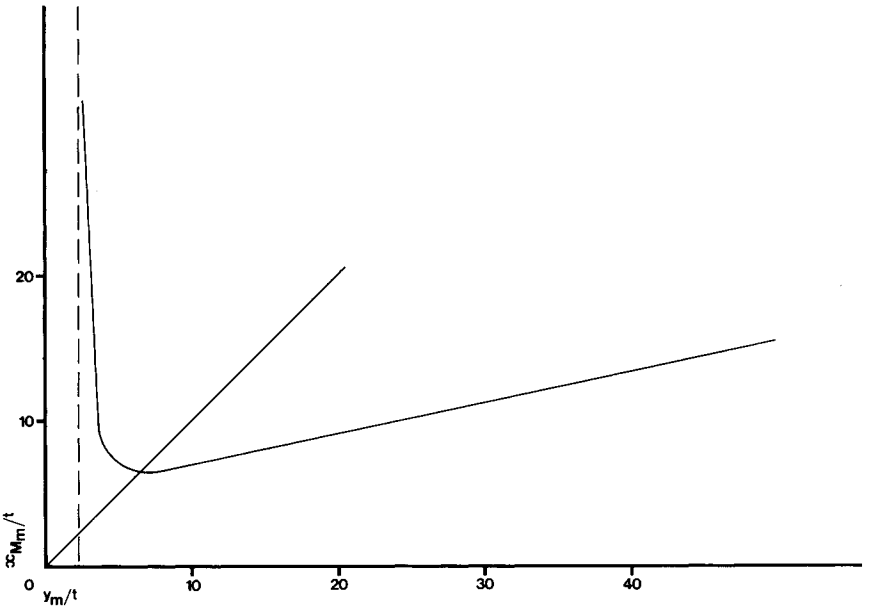

Fig. 10. Dimensionless x_{M_m}–y_m relation for a plastic legged adhesive.

For all $y_m/t >$ (say) $6^1/_2$, $x_{M_m} < y_m$, in direct contrast to the result for an elastic adhesive, eq. (37). Practical cases tend to have $y_m/t > 20$, when x_{M_m} is predicted as $\lesssim y_m/2$. This accords reasonably with observations, giving $x_{M_m} < 0.25$ mm for 0.025-mm tapes, which agrees with the unmagnified visual observation of total 90° bending but with an $(R_u)_f$ much greater than the radius at the point of bending.

The fully plastic theory also provides a very direct explanation of the increase in peel force with rate observed in such studies as those of Wong[16] (at least in his "C region", between two zones of stick-slip behavior, vide infra, in which he describes the adhesive as behaving with "retarded high elasticity," i.e., without the viscous flow possible at lower rates, but not yet elastically) and Gardon.[17] Since eq. (38) requires $P \sim \sigma_y$ at constant t (unless y_m changes dramatically), the observed increases of P with rate follow immediately from the well-known increase of the *yield* strengths of the polymers used in P.S. tapes, with rate (see, e.g., refs. 10 and 11). It is not necessary to seek for increases in adhesive ultimate strengths, in forces of adhesion, or in other energy dissipation mechanisms, with pulling rate. The increase of adhesive yield strength alone will cause P to rise with increasing rate, until either the true interfacial force of adhesion is exceeded or the rate becomes high enough to cause elastic behavior of the adhesive, at the high-rate "noisy unwind" stick-slip transition, which is discussed in more detail below.

The linear dependence of peel force on adhesive thickness required by eq. (38) also holds for the literature data, provided that the rates are ap-

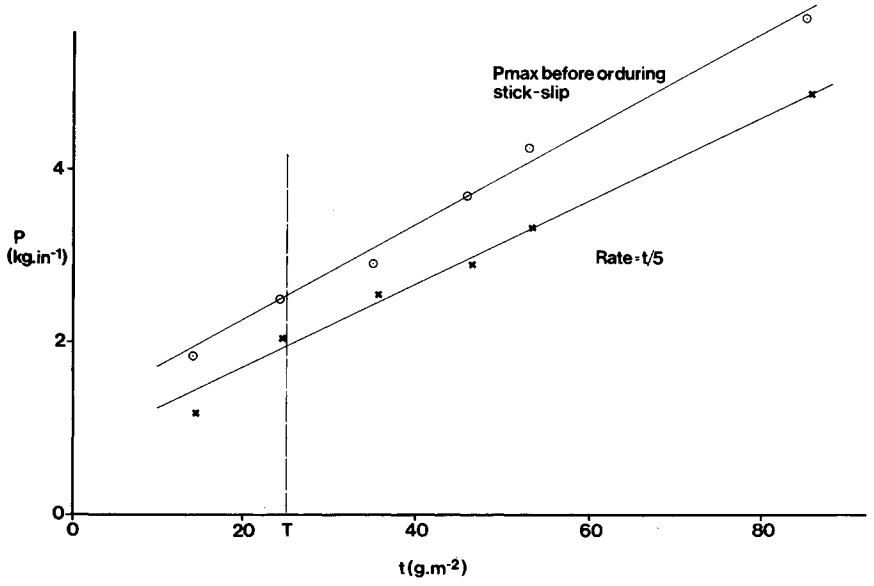

Fig. 11. P–t relations for selected data of ref. 9, Fig. 7. See text; all failures cohesive.

propriately selected so that the rate of straining of the *adhesive* is constant and independent of t. The data of Figure 7 of Aubrey et al.[9] are replotted in Figure 11 (lower line), taking peel force values shown for rates arbitrarily selected as $t/5$ (in units of cm/min and g/m^2). In this way, the machine rates being proportional to glueline thicknesses, the effective straining rate of an element of adhesive was the same for all points plotted.

The data of Gardon's[17] Figure 5 are similarly replotted in Figure 12 for two rates, $t/15$ (upper curve) and $t/50$ (in units of g/in. and μ). In each case, linearity is satisfactory at least for $t \gtrsim T$. The vertical lines in the figures indicate the approximate magnitudes of T. The deviations for $t \ll T$, suggested in Figure 11 and evident in Figure 12, and the nonzero intercepts of the extrapolated linear portions of the plots at $t = 0$ are obviously due to the neglect in the derivation of eq. (38) of the contribution to peel force of the work loss in the plastic bending and unbending of the adherend, and to the inability of very thin gluelines adequately to support the full length of the plastically yielding zone of adherend or to tolerate the resulting shear. The intercept on the P axis, in fact, provides a measure of the contribution of the irreversible work term to peel force, at least as far as work lost in the adherend is concerned.

Thus, when applied to the adhesive as well as to the adherend, even a very crude plastic theory has been shown to accord better with the facts than does its (even partially) elastic equivalent. Although, as already pointed out, the true behavior of an adhesive in "legging" peel probably shows both elastic and plastic character and the rate dependence of adhesive properties has not been fully analyzed, it is nonetheless clear that the

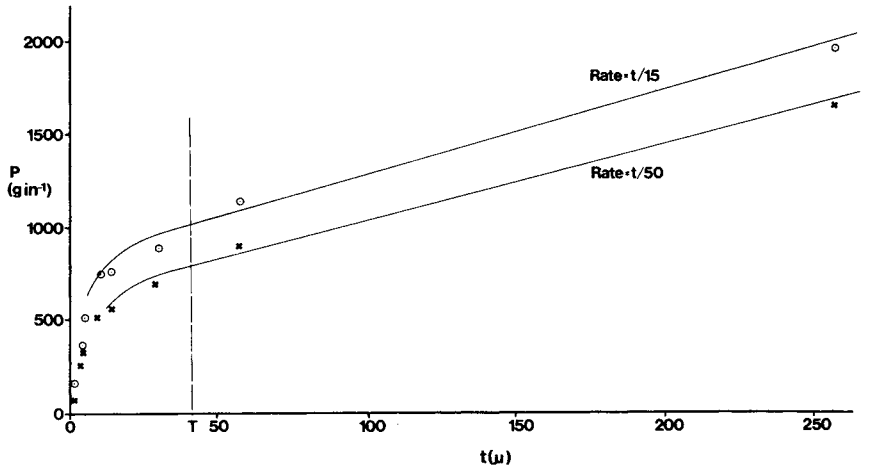

Fig. 12. Variation of P with t for rates proportional to t. Data of ref. 17, Fig. 5. All failures cohesive.

neglect of the potentially plastic character of both adherends and adhesives has led to serious inadequacies in the classical theories of peel. In consequence, these classical theories apply to peel of only a very limited range of practical bonds and give grossly misleading results in very many cases. Generally, the classical theory severely underestimates the toughness of bonds under peeling or cleaving conditions. Development of a full theory of equilibrium peeling will be an extremely complex task, since allowances must not only be made for inelasticity and rate dependence of both adherend and adhesive and the varying values of R_u in the bonded zone, but also for the finite lengths of adherend over which some yielding occurs in both bending and unbending, the varying depth of penetration of plasticity into the adherend thickness when $M_y < M < M_p$, and the associated influence of tensile loads on flexural moments of resistance (see below), the varying angle of the legs to (both) adherends, and the form of lateral contraction of the legs during extension. Even a computer solution may yet require some approximations.

Nonetheless, the difficulties of obtaining the full plastic or plastic/viscoelastic solution do not justify continuation of the evidently false assumptions of widespread substantially elastic behavior, in view of the clearly superior fits to the empirical facts which can be provided by even the very elementary plastic assumptions made herein.

PLASTICITY IN STICK-SLIP PEELING

Finally, two cases of nonequilibrium behavior during peeling may be mentioned, the explanations of which appear to be critically dependent upon the assumption of plastic behaviors. Aubrey et al.[9] and Gardon[17] have both observed low-rate stick-slip behavior when peeling bonds to

adhesives of high elongation, and Wong[16] has observed a second higher-rate region of stick-slip peeling, showing a rather different form of force–time relation during its oscillations. The maximum forces encountered in the work of Aubrey et al. during the (metastable) phase of stick-slip peeling when low-rate adhesive behavior obtains are ca. $5^1/_2$ kgf on 25 × 0.025 mm adherends, and about $2^1/_2$ kgf when the thickness is reduced to 0.015 mm. The corresponding forces which would have caused purely tensile adherend yield are respectively 7.2 and 4.3 kgf. Tensile forces near to yield cause reductions of the moment of resistance of the stressed adherend toward flexural yield; it can be considered that the thickness of the adherend is reduced in proportion to the fraction of the tensile yield load which is being borne, entirely by adherend "fibers" on the outside (tensile) face of the bend. The adherend M_y is thus reduced to that defined by an "effective thickness":

$$T_{\text{eff}} = T\left(1 - \frac{P}{S_y b T}\right). \tag{49}$$

The two maximum loads give very similar values for T_{eff} (respectively 0.006 and 0.007 mm) and thus also for $(M_y)_{\text{eff}}$ at the moment of transition to faster-rate (weaker) behavior of the adhesive. This could suggest that the transition is moment controlled. In any case, the maximum force in such stick-slip peeling will clearly have caused much more extensive plastic bending (due to the reduction of M_y by the tensile load) than predicted from the simple plastic theory, and the rise in effective adherend M_y as the change to higher-rate behavior of the adhesive leads to reduction of P may well contribute to controlling the onset and stability of the observed oscillations.

However, it is very probably significant that onset of this type of stick-slip seems to occur at a constant rate of adhesive strain, independent of t or P. This may be seen from Figure 13, in which the data of Figure 7 of Aubrey et al.[9] are replotted to show the linear dependence of machine rate for stick-slip onset, upon t, as required for onset at constant adhesive strain rate. The effect of varying adherend thickness (T) upon rate for stick-slip onset (or P at onset) is much less (ref. 9, Fig. 8), so the onset is most probably controlled by a rate-determined change in adhesive properties, with adherend partial tensile yield contributing mostly to oscillation stability.

Combination of proportionality between onset (machine) rate and t (Fig. 13) with linear dependence of P upon t at equal adhesive straining rates, eq. (38) and Figures 11 and 12, leads to a linear dependence of peel force at stick-slip onset upon t. This is observed, as in the upper plot of Figure 11, showing good linearity.

The higher-rate form of stick-slip peeling, the well-known "noisy unwind," can occur with most pressure-sensitive tapes. Noisy unwind has been shown by Wong[16] to occur over a range of rates between those for which the adhesive behaves with "retarded high elasticity" (and where

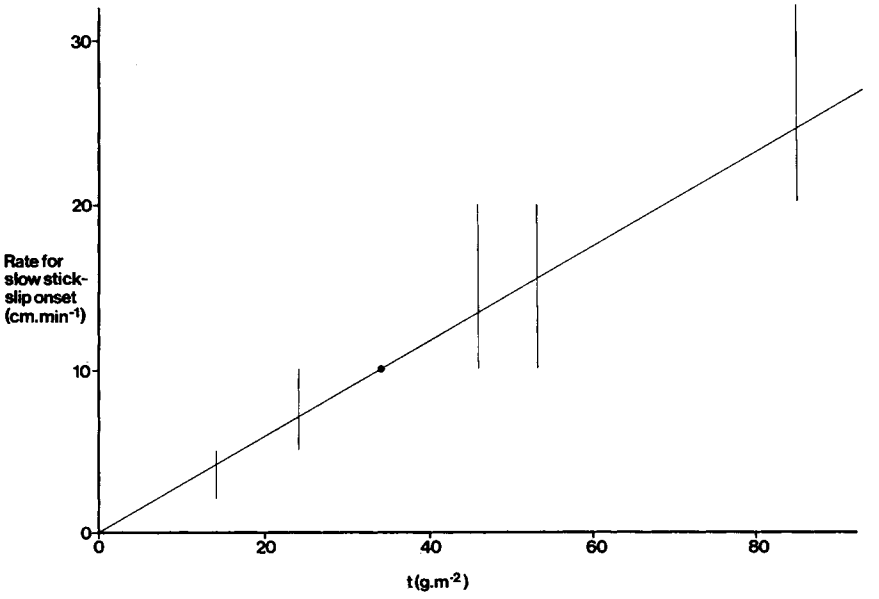

Fig. 13. Dependence of rates within which onset of slow stick-slip occurs, upon adhesive thickness. Data of ref. 9, Fig. 7.

peel forces are high) and those (higher) rates at which the adhesive behaves substantially elastically, and supports a much lower peel force. After such stick-slip peeling, the peeled adherend exhibits a regular series of transverse lines, increasing in spacing substantially linearly as the free length of adherend increases (Fig. 14). Wong[16] attributed these lines to zones of strained adhesive, but microscopic examination (See Figs. 15 and 16) shows that they are in fact points of localized plastic yielding which have been largely (but not completely) plastically unbent. This has been verified by examination of tape stopped during such "noisy unwind" peeling, and of peeled lengths of tape after such peeling when lightly rebonded to glossy surfaces—the plastically yielded kinks show up as linear air bubbles under the film (Fig. 16). The short lengths of peeled tape between these yielded kinks seem to be substantially unbent. At the stage of maximum plastic bending during such stick-slip peeling, the adherend is more acutely bent at the plastic hinge than it is during steady peeling at somewhat lower rates (compare Figs. 1 and 15).

Further empirical facts with which any theory of such noisy unwind must accord are as follows. At rates above the stick-slip region, peel occurs at very low P and *without* adherend plastic yield. This latter point has been verified, assuming that the time–temperature superposition principle continues to apply (as it was shown to do by Wong[16]) by fast peeling of cooled samples (see Fig. 17). Also, peel forces (P_C) in the slower region (below the stick-slip rate zone, i.e., Wong's region C) are[16] much greater than those (P_E) in the faster region above stick-slip, which Wong

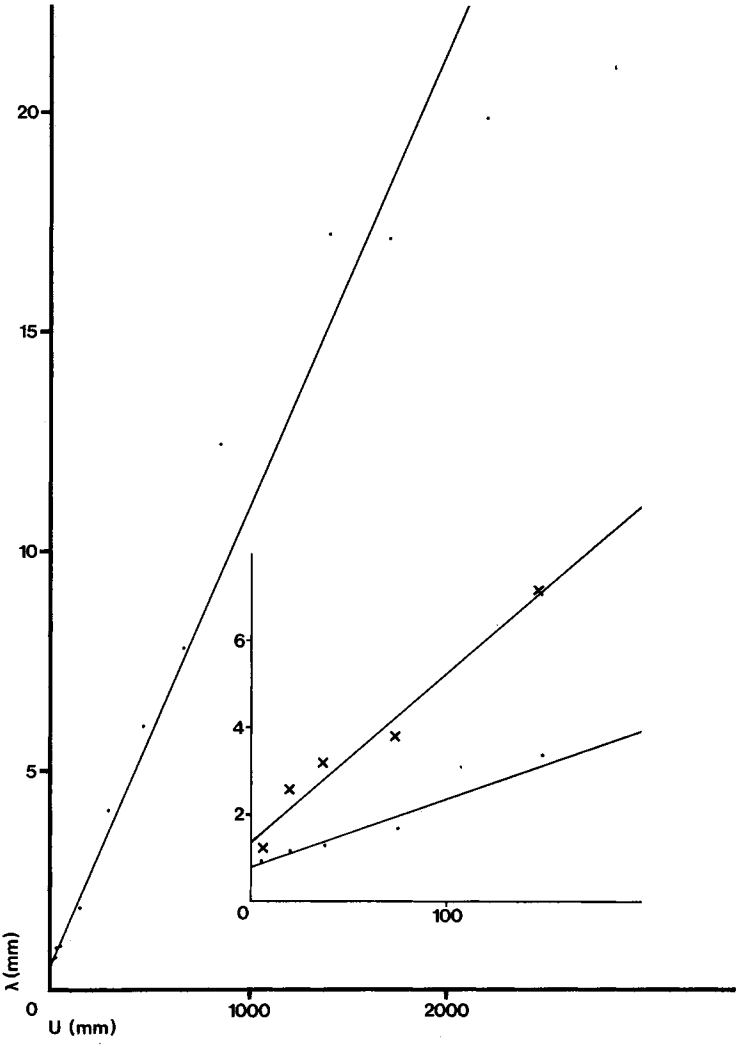

Fig. 14. λ–U relations for noisy unwind.

calls region E and in which he regards the adhesive (also) as behaving substantially elastically. The relation $P_C \gg P_E$ also follows from theory, if plasticity of both phases is assumed for the C region and elasticity (at least of the adhesive) for the E region, by combining eqs. (38) for P_C and (12), noting $P_E \not> P_0$.

At equal rate, $(\sigma_y)_{\text{plastic}} = (\sigma_m)_{\text{elastic}}$, so the condition for $P_C > P_E$ is

$$t\beta \ln\left(\frac{y_m}{t} + 1\right) > 1. \tag{50}$$

For the data of Aubrey et al.,[9] Wong,[16] or the experimental section herein, $t \doteq T$; and at rates high enough to cause elastic adhesive behavior, $Y \approx E$. Thus,

$$\beta^4 (= 3Y/ET^3t) \approx 1/t^4 \tag{51}$$

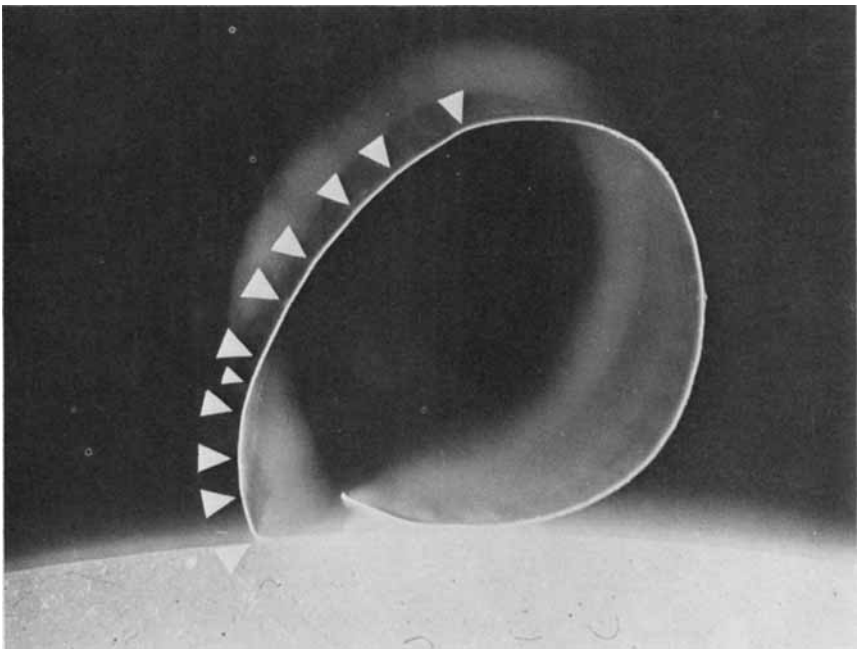

Fig. 15. Photograph of adherend peeled by noisy unwind; pointers mark kinks.

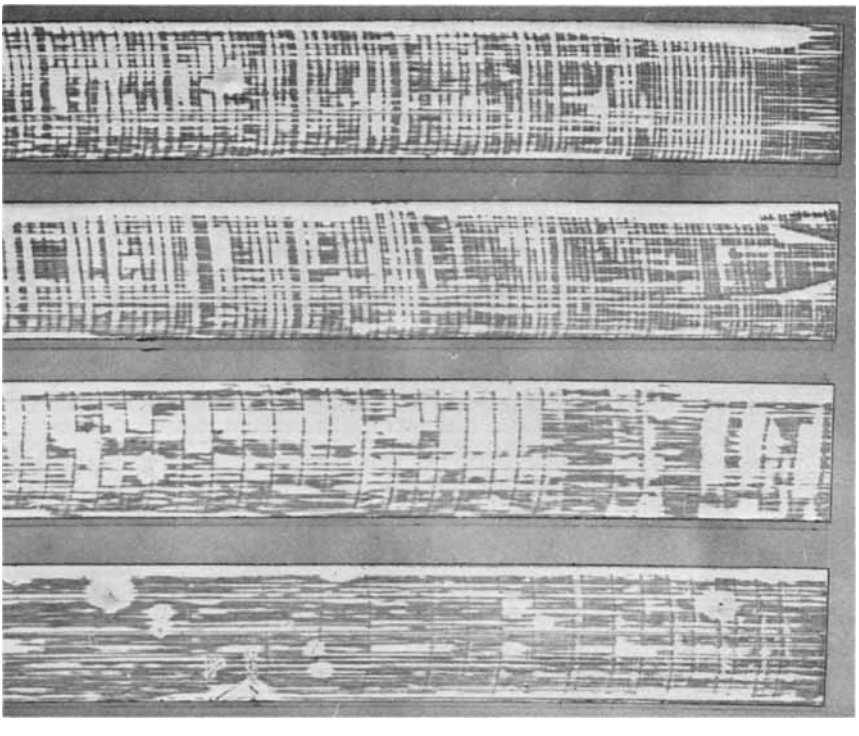

Fig. 16. Photograph of adherend peeled by noisy unwind, lightly rebonded to a glass plate.

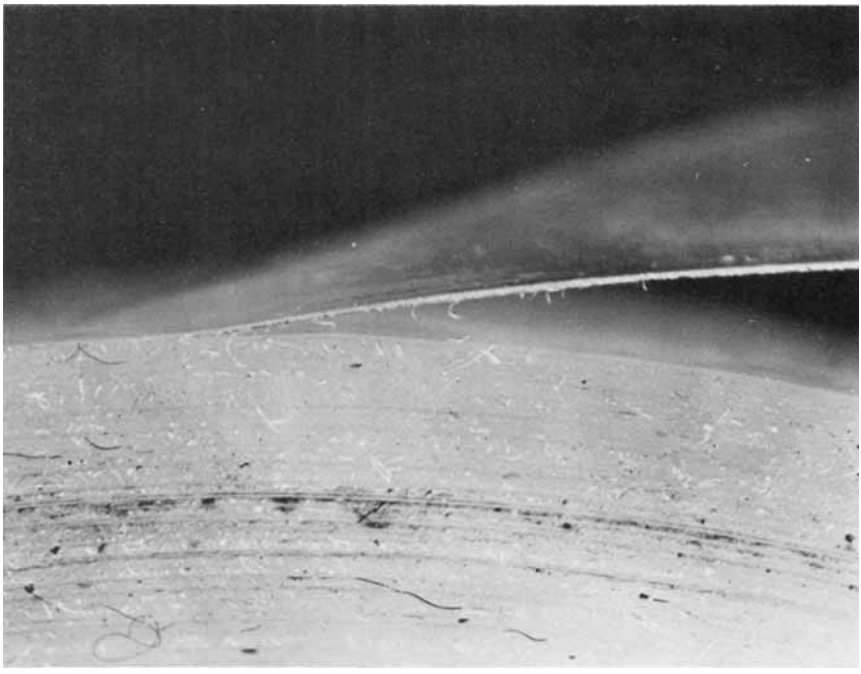

Fig. 17. Photograph of tape peeled in Wong's "E" region, at circa −5°C, showing no adherend yield.

and since y_m in the plastic region $\approx 10t$, the required condition (50) is fulfilled even for the *maximum* possible value of P_E when $L_0 = 0$. As L_0 increases with elastic behavior, P_E, of course, rapidly decreases further.[13]

The sudden fall in P after a slow rise, which occurs during noisy unwind,[16] can be associated with a transition from plastic to elastic adhesive behavior. This is enforced by completion of bending around a localized plastic hinge to near 90° (after which the peeling rate, previously less than machine rate as the tape progressively bent, must rise to equal the machine rate), combined with a rise in P (and of the associated stored energy in the tape due to the tensile load) to a level greater than that which can be borne by the existing adhesive legs. The consequent failure of these legs leaves an overstressed adhesive zone, which must then fail *elastically* at rates faster than machine rate, P therefore falling rapidly until the stored energy is dissipated. P can then begin to rise again, causing bending of the tape around a new hinge supported by an adhesive now again behaving plastically. The full cycle for all of the major joint parameters is followed through one cycle of noisy unwind (Table III).

After the stage of fast crack propagation in elastic adhesive, L_0 is significantly greater than zero, so that initially elastic and later plastic adherend bending can occur around $x = x_{M_m}$ under low P. As a result of the rotation of the loaded adherend between $x = 0$ and x_{M_m}, the rate of stressing of the adhesive stays well below machine rate and the adhesive fails plasti-

TABLE III
Stages in High-Rate Stick-Slip Peeling[a]

Stage	I	II	III	IV	V	VI
Joint form		→			→	
θ	~0°	Low, rising slowly	High, rising fast	90°	~90°	"90°" at old hinge, ~0° at x_{M_m}
Rate, relative to machine	$\ll$	$\ll$	$\ll$	Increases to $\doteq$	Increases to >, as legs fail to bear P	>
Plasticity						
Adherend	E	P	P	P	P	E
Adhesive	P	P	P	P	→E	E
Legs	very short, starting to form	some	many	many	rupture starts	nil
Energy store	$\doteq 0$	increasing	increasing fast	increasing fast	maximum	dissipating
P	minimum	rising	high, rising fast	high, rising fast	maximum	decreasing rapidly, to $(P_0)_{\text{elastic}}$
$\therefore q$	low	rising	still rising	near-static	equilibrium breaks down: x_{M_m} starts to shift, toward $\pi/4\beta$[b]	negligible (non-equilibrium)
Legs able to bear P?	√	√	√	√	×	×
M_m	$<M_p$	M_p	M_p	balanced by legs	ambiguous (nonequilibrium)	$<M_p$
$\therefore m$	high	decreasing	decreasing fast	low, near, static	starts increasing fast	increasing fast
x_H[b]	q	~q	$<q$, decreasing	→0	hinge shifting	hinge shifting
$\therefore L_0$	~m	decreasing	low, decreasing fast	~0	decreases, as glue-line edge starts to shift	increasing fast
Adhesive crack propagation	nil	nil	nil	nil	initiates via leg rupture	fast

[a] m = Moment arm of P about x_{M_m}, the "hinge point", q = length of adhesive, along x axis, which bears the load P, lying between the glue-line edge on the fixed substrate and x_{M_m}, x_H = distance parallel to x-axis, from the glueline edge on the peeling adherend, to x_{M_m}; L_0 = moment arm of P about the glueline edge on the peeling adherend, $= m - x_H$.

[b] When the adhesive is elastic, x_H $(= q) \doteq \pi/4\beta$ if L_0 is low, but as L_0 increases, $x_H \to 0$. When the adhesive is plastic the hinge is at x_{M_m}, $= q$ until the contribution of the legs to restoring moment becomes significant.

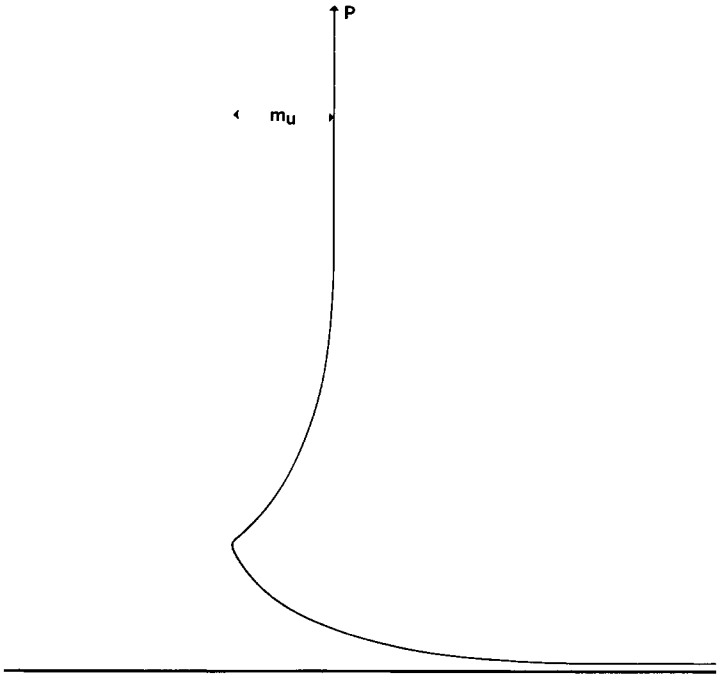

Fig. 18. Configuration of peeling adherend during noisy unwind, after formation of first full hinge.

cally. As rotation proceeds about an almost-fixed hinge point (this, in fact, shifting at L_0 decreases, from near $x = 0$ to remain at the current $x_{Mm} = q$), L_0 falls and P thus rises, supported by a somewhat increasing length of more highly extended adhesive. As a result, M_m is kept approximately equal to M_p, until a configuration of the type of Figure 8 is reached. Thereafter, P may continue to increase for a limited time without further major change of joint configuration (stage V, Table III), more strain energy being stored in the free length of adherend, until rupture of the outer legs initiates elastic adhesive failure. Until this occurs, the moment around x_{Mm} due to P is largely counterbalanced by that due to the legs, which keep the hinge point substantially stationary. After elastic adhesive failure has started, a new hinge point is established within the glueline adjacent to the new glueline edge (where fast crack propagation in the temporarily elastic adhesive stops), at the required x_{Mm} ($<\pi/4\beta$) from the new $x = 0$. The new L_0 is fixed by the distance between the old hinge, now a near-90° kink in the free adherend and the new glueline edge. As rotation occurs about the new hinge, the configuration of Figure 18 develops, and as the old hinge transmits steadily increasing loads at increasing values of θ, ultimately $P \cdot m_u$ reaches M_y, and the old hinge is largely unbent. The resulting "flapping" of the free adherend, as it alternates between the configuration of Figure 18 and approximately that of Figure 8 (or IV in Table III), results in the noise heard in noisy unwind. The

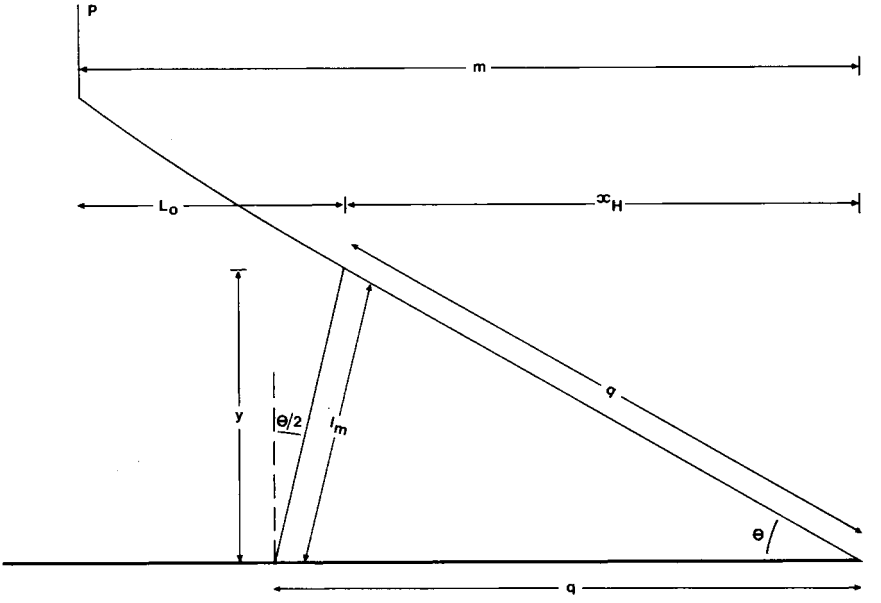

Fig. 19. Geometry of "rigid hinge" peel.

frequency of the sound heard is approximately that expected from the determined frequency of kinks found in the peeled tape.

Analysis of this theory for noisy unwind fits the observed data well. The variation of P during phases I to IV (Table III) is controlled by plastic behaviors, and the value of the wavelength (λ) between "kinks," by essentially the elastic behaviors during stage VI. If we assume, as is empirically substantially true, that the point of maximum moment does not shift during most of the rotation of each successive step of peeling adherend as a "rigid hinge," then the load-bearing length of adhesive (q) is constant, and the failure-zone geometry is as in Figure 19.

M_m ($=M_q$) must also be constant. $P = M_p/m$, and for the $L_0 = 0$ case,

$$m = q - l_m \sin(\theta/2) \tag{52}$$

$$l_m = 2q \sin(\theta/2) \tag{53}$$

and

$$\theta = \sin^{-1}(y/q). \tag{54}$$

Combining (52), (53), and (54),

$$P = M_p/m = M_p/q[1 - 2 \sin^2 {}^1/_2 \sin^{-1}(y/q)]. \tag{55}$$

The form of function (55) is plotted in Figure 20. The P–y dependence it implies is not dissimilar to that found for the noisy unwind region by Wong (ref. 16, his Fig. 8-lb and region D, a typical P–y trace from which is drawn, arbitrarily superimposed, onto Fig. 20). The curve contrasts markedly with that found by Wong for the slower rate stick-slip (his

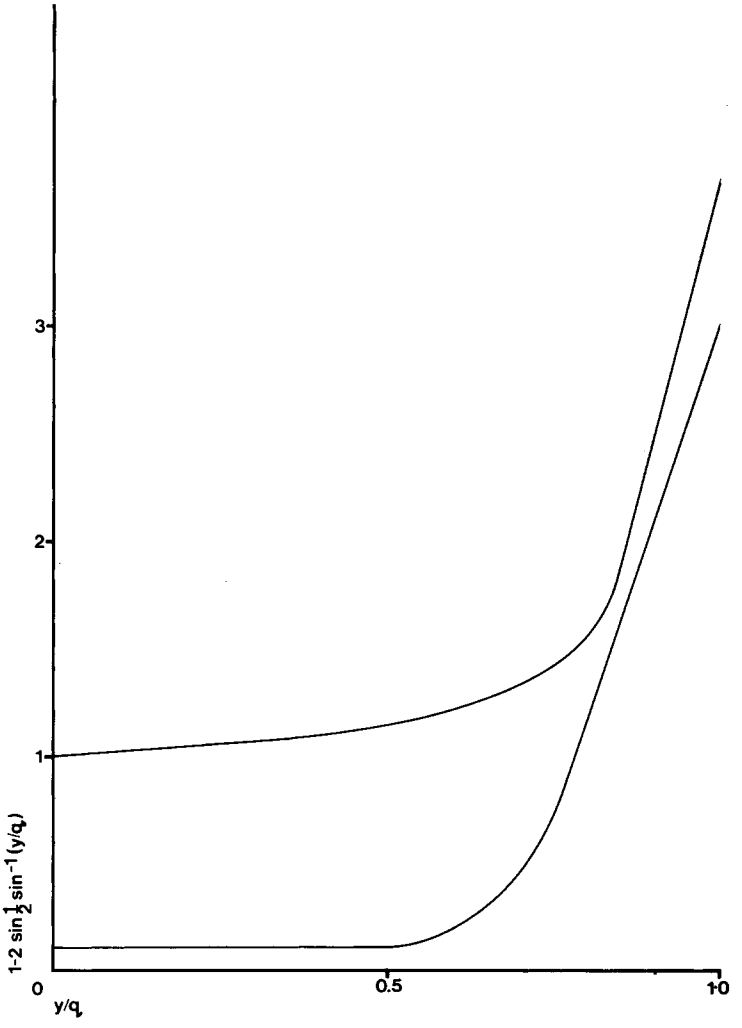

Fig. 20. P–y dependences, from theory and practice,[16] for noisy unwind.

region B), where the P–y traces are convex upward, confirming the appropriateness of this stick-slip mechanism to the faster form only of such behavior. (The excessive loads predicted for early stages of the cycle by this model are, of course, because adherend plasticity does not, in fact, develop until either P or L_0 is significantly above zero.)

The form of the fall of P after the maximum, being associated with a sharp rise in L_0 from $\doteq 0$, can be expected to be a more rapid form of that found during such "F type" failure in our previous work.[6]

When the free length of adherend (U) is significant, the form of Figure 20 changes, the rate of increase of slope at higher P being ameliorated as such loads cause greater (elastic) straining of such free adherend. The ultimate form of the P–y relation at very high U will be a straight line.

The λ value is determined from a combination of a minimum value equal to x_{M_m} with the adhesive elastic, the adherend *just* yielding ($M_m = M_y$), $L_0 = 0$, and a second term due to the finite initial value of L_0 after the rapid crack propagation during phase VI (Table III), which is proportional to the stored strain energy released. For the former term, combining (1) and (12),

$$\lambda = m = M_p/P_0 = \beta S_y T^2/2\sigma_m. \tag{56}$$

Equation (56) gives $\lambda \approx 1$ mm for the tape of the experimental herein (q.v.), as found. The component of λ due to stored energy must equal the elongation of the free adherend length U just before the rapid failure phase VI, $= P_m U/EbT$. For our data, this predicts a slope of λ versus U of the order of 10^{-2}, as found (Fig. 14). The experimental observation that the spacings of kinks, λ, do increase linearly with U but that the plot does *not* show a zero intercept on the λ axis is in itself strong evidence for the correctness of the theory of noisy unwind developed above.

EXPERIMENTAL

This study used a commercially available sticky tape ("Holdfast," of Johnson Dickinson & Co.), based on a regenerated cellulose film, $T = 0.038$ mm, $b = 12$ mm, $S_m = 10.5$ kgf/mm^2, $S_y \approx 5.0$ kgf/mm^2, $J_m = 0.25$, $J_y \approx 0.005$, $E \doteq 600$ kgf/mm^2 (all determined at 5 mm/sec). The adhesive was a natural rubber/hydrocarbon copolymer resin type. At low rates, $\lesssim 10$ mm/sec, $P = 0.6$ kgf; and since $M_p = 0.022$ kgf·mm (yielding $m = 0.03$ mm for a nonlegged situation, which is $\approx T$ and thus corresponds to an even sharper right-angled peeling than is in fact observed), most of P is supported by adhesive legs, which also counterbalance most of the moment due to P. (Similar calculations on the data of low-rate peel in Aubrey et al.[9] or Gent[10,11] show that adhesive legs must counterbalance much of the moment due to P, since otherwise $m \lesssim T$, corresponding to a more extreme form of plastic adherend collapse than is ever actually observed, and also $m \ll x_{M_m}$, which $= \pi/4\beta$ since $L_0 = 0$, which is impossible.)

Noisy unwind occurred with this tape at rates around 10^3 mm/sec and mean $P \sim 0.3$ kgf. Figure 15 shows the tape stopped during such unwind, and Figure 16, a sample of the so stripped adherend rebonded lightly to a glass plate. These figures illustrate the kinking of the adherend and the extent of subsequent unbending of plastic hinges. When cooled to -5°C before peel at $\gtrsim 10^3$ mm/sec, the tape peeled without any sign of plastic yielding (see Fig. 17), $P \doteq 0.02$ kgf (Wong's "E" region behavior).

Various lengths of tape were peeled continuously, at circa 1500 mm/sec and from initial free adherend lengths $U_i < 5$ mm. Mean wavelengths λ between kinks were determined at intervals along the peeled adherends and are plotted for three runs in Figure 14; each plot is linear and shows a finite λ intercept, although the slopes and intercepts vary with rate and U_i.

SUMMARY AND CONCLUSIONS

By recognizing the limitation imposed on moment maxima by the possibility (and occurrence) of adherend plasticity in flexure, and also of the possibility of plastic extension of the adhesive, a much more complete picture has been obtained of the dependence of the configuration of peeling adhesive joints upon the dimensions and strengths of their component materials. The dependences of peel forces P on the same parameters has also been shown derivable once the factors controlling the adoption by a peeling joint of particular geometries have been identified. The effect of peeling rate upon joint configuration and upon P arise largely from its influence upon the effective stress–strain behaviors exhibited by the adhesive, as has been shown by Gent[10,11] to be predictable from consideration of stress–strain behavior of the free adhesive at appropriate rates. Equation (38) herein emphasizes the need to compare peel behaviors for joints having differing adhesive thicknesses t at equal effective rates of straining of the adhesive (machine rate proportional to t); and, provided this is done, literature data has been shown to reduce simply to fit a linear P–t law, as required by eq. (38). Rate-induced transitions between types of peeling behavior (e.g., ref. 9) appear to occur at constant rates of adhesive strain, and the stick-slip behavior of joints in transitional (rate) regimes has been shown deducible by considering the interplay of elastic and plastic behaviors of both component materials in the joint, during alternations of the effective straining rates in various zones in the joint.

In conclusion, it is instructive to consider the overall dependence of peel force P upon adherend thickness T which can now be predicted from a combination of all of the forms of behavior considered herein. Figure 21 shows this schematically for an "ideal" adhesive, capable both of showing sufficiently high (and plastic) elongations to permit a thin adherend to adopt the "legging" peel configuration of Figure 8, and also having sufficient

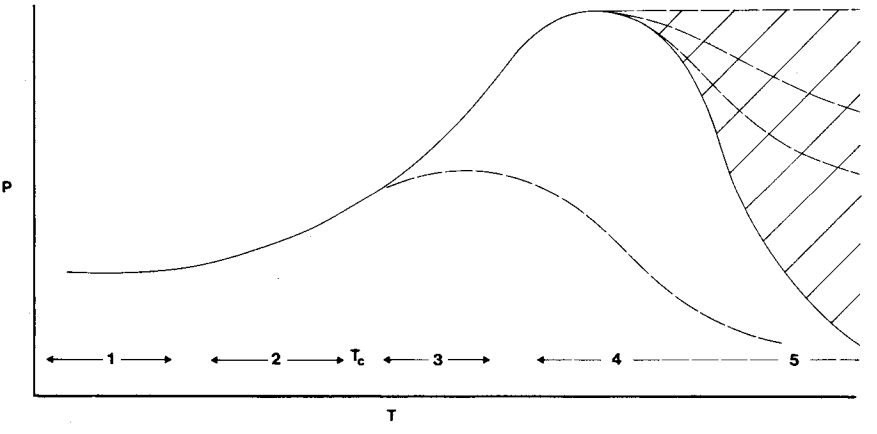

Fig. 21. Schematic variations of P with T, for an "ideal" adhesive; see text.

cohesive and adhesive strengths to support elastic peel of much thicker adherends, at low values of θ. While it is improbable that any real adhesive can show the complete range of behaviors of Figure 21, many joint types have been described as showing typical parts of such a P–T trace. Thus, the required substantial independence of P of T in region 1 has been observed by Aubrey.[9] In this region, the controlling equation is eq. (38). As T increases, after a transitional region in which legging becomes much less significant, the $T^{2/3}$ law of eq. (23) applies in region 2. *If* region 4 behavior does not intrude due to limitations imposed by test machine or sample size restrictions (dashed lines), then this region is succeeded, as T_c is exceeded, by a zone of elastic peel (region 3), where the Yurenka equation (eq. (7) herein) applies, and $P \sim T^{3/2}$ at constant L_0.

The increase of P with T is ultimately limited either by inadequacy of adhesive adhesion or, probably more commonly, by the ability of joint configuration actually tested (or ruptured in service) to impose increasing moment arms m or L_0 as peel or cleavage proceeds, rather than permitting equilibrium peel under constant geometric conditions, as occurs with thinner substrates. Sharply decreasing traces of P versus time, after onset of peeling, are then observed, as in case F of our previous paper. The controlling equation for region 4 is still Yurenka's equation (eq. (7) herein), but it is being applied with nonconstant L_0, controlled by the test geometry as T is increased. Thus, the net effect of increase of M_0 and of L_0 leads to a decline of P or at minimum to a decreased rate of increase of P, with increasing T, but the form of the P–T curve is not universal in this region, depending as it does upon the geometric constraints imposed by the total joint rupture situation. The limiting low P case of region 5 is ultimately obtained for high T *if* L_0 can increase almost indefinitely, $P \rightarrow 0$ as predictable from the Yurenka eq. (7), but failing this condition P remains finally at a higher, nonzero value as indicated by the dotted lines in region 5.

The P–T maxima observed by Mylonas[7] would seem to lie in regions 3 and 4 (and possibly 2, or 2 and 4, if 3 is elided in his case). Johnson's plots[18] (his Figs. 4 and 7) show at least regions 2 to 5 (L_0 limited).

Recognition of the crucial and interlinked roles of moment limitation, of potential plasticity of both joint materials, and of effective rate of straining of elements of adhesive thickness seem to permit a much more comprehensive understanding of peel behavior than has previously been possible. Further work is clearly required, at minimum upon the effects of nonnormal peel forces (variation of peel angle, e.g., as in 180° strip-back), on the superposition of adherend tensile (partial) yield upon adherend flexural yield, upon plastic micromechanics (and geometry) within the load-bearing zones of peeling joints,* on more rigorous assessment of behavior of plastic adherends bonded with viscoelastic adhesives, and

* A recent publication[19] has reported the first work in this direction, showing a proportionality between peel force and depth of penetration of plasticity into an adhesive phase, P being controlled by energy of inelastic deformation.

particularly on the use of the theories already derived, in design calculations.

APPENDIX

Since submission of the above for publication, the referee has drawn the author's attention to a recently published study,[20] which provides a computer-solvable analysis for the condition of a plastically bent peeled adherend, without plastic unbending (or legging). Chen and Flavin[20] distinguish, in their key equation (their eq. (8)), between the radius at the cleavage point under the peeling load (their ρ), and the unloaded $(R_u)_f$. However, as $M_0 \approx M_p$ for stable peel-with-yield, $\rho \doteq (R_u)_f$ and their eq. (8) reduces to

$$P = S_y bT\,(T/R_f - 3S_y/2E)/4$$

For the data of our previous work, the second term is negligible, so this reduces to eq. (10) herein. The latter of course fits all of the data of ref. 6, Figures 5 and 6, and of Figure 7 herein, $P_{\text{observed}}/P_{\text{calc}}$ having a mean value of 0.87 with standard deviation 0.40. The data of Figure 7 herein, alone, have mean $P_{\text{observed}}/P_{\text{calc}}$ 1.05, standard deviation 0.23. Both analyses, although proceeding from differing starting points, agree as to the key role of adhesive strain energy density to rupture, and the greater resistance to peel imparted by adherend plasticity. However, the two approaches have given rise to differing explanations of the maxima sometimes observed in P-T curves (e.g., ref. 7), and this point may require further study.

The author wishes to thank Ciba-Geigy (U.K.) Limited for the facilities to complete and write up this piece of private research, arising from an earlier interest, and also Dr. D. W. Aubrey and Mr. M. Sherriff for helpful discussions. Some of the conclusions of this work were reported at the International Rubber Conference, Brighton, U.K., 1972.

References

1. G. J. Spies, *Aircraft Eng.*, 64 (March 1953).
2. C. Jouwersma, *J. Polym. Sci.*, **45**, 253 (1960).
3. D. H. Kaelble, *Trans. Soc. Rheol.*, **4**, 45 (1960).
4. J. L. Gardon, *J. Appl. Polym. Sci.*, **7**, 643 (1963).
5. J. Case and A. H. Chilver, *Strength of Materials and Structures*, 2nd ed., E. Arnold, London, 1971, pp. 264–5.
6. A. J. Duke and R. P. Stanbridge, *J. Appl. Polym. Sci.*, **12**, 1487 (1968).
7. C. Mylonas, in *Proc. 4th Int. Congr. Rheol.*, R. H. Lee, Ed., Providence, Rhode Island, 1965, pp. 423–447.
8. J. J. Bickerman, *J. Appl. Polym. Sci.*, **2**, 216 (1959).
9. D. W. Aubrey, G. W. Welding, and T. Wong, *J. Appl. Polym. Sci.*, **13**, 2193 (1969).
10. A. N. Gent and R. P. Petrich, *Proc. Roy. Soc.*, **A310**, 433 (1969).
11. A. N. Gent, *Bull. Soc. Chim. France*, 3237 (1970).
12. D. H. Kaelble, *Trans. Soc. Rheol.*, **3**, 161 (1959).
13. S. Yurenka, *J. Appl. Polym. Sci.*, **6**, 136 (1962).
14. D. H. Kaelble, *Trans. Soc. Rheol.*, **9**, 135 (1965).

15. Reference 5, p. 154.
16. T. K. M. Wong, Thesis: Peel Adhesion of Pressure-Sensitive Tapes, National College of Rubber Technology, 1971.
17. J. L. Gardon, *J. Appl. Polym. Sci.*, **7**, 625 (1963).
18. J. Johnston, *Adhesives Age*, 20 (April 1968).
19. H. E. Bair, S. Matsuoka, R. G. Vadinsky, and T. T. Wong, *J. Adhesion*, **3**, 89 (1971).
20. W. T. Chen and T. F. Flavin, *I.B.M. J. Res. Develop.*, **16**, 203 (1972).

Received March 26, 1974
Revised April 15, 1974